Proximity-labeling proteomics reveals remodeled interactomes and altered localization of pathogenic SHP2 variants

Anne E. van Vlimmeren[1,2], Lauren C. Tang[2], Ziyuan Jiang[1], Abhishek Iyer[2], Rashmi Voleti[1], Konstantin Krismer[3], Jellert T. Gaublomme[2], Marko Jovanovic[2], Neel H. Shah[1,4*]

[1] Department of Chemistry, Columbia University, New York, NY 10027

[2] Department of Biological Sciences, Columbia University, New York, NY 10027

[3] Koch Institute for Integrative Cancer Biology, Massachusetts Institute of Technology, Cambridge, MA

[4] Herbert Irving Comprehensive Cancer Center, Columbia University, New York, NY 10032

* corresponding author: neel.shah@columbia.edu

Keywords

SHP2, tyrosine phosphatase, protein-protein interaction, phosphotyrosine, mitochondria, TurboID

Abstract

Missense mutations in *PTPN11*, the gene encoding the protein tyrosine phosphatase SHP2, are common in several developmental disorders and cancers. While many SHP2 mutations disrupt auto-inhibition and cause hyperactivity, several mutations do not enhance catalytic activity. Both activating and non-activating mutations could potentially drive pathogenic signaling by altering SHP2 protein-protein interactions or subcellular localization. We employed proximity-labeling proteomics to map the interaction networks of wild-type SHP2, ten clinically-relevant mutants, and SHP2 bound to an inhibitor that stabilizes its auto-inhibited state. Our analyses revealed mutation- and inhibitor-dependent alterations in the SHP2 interactome, with several mutants also showing changes in localization. In particular, some mutations had increased mitochondrial localization and impacted mitochondrial function. This study provides a rich resource for exploring SHP2 signaling and offers new insights into the molecular basis of SHP2-driven diseases. Furthermore, this work highlights the capacity for proximity-labeling proteomics to detect missense-mutation-dependent changes in protein interactions and localization.

Introduction

Missense mutations are a prevalent type of genetic variation across the human genome, and they often play a causal role in human diseases[1,2]. Missense mutations in proteins frequently change protein function by directly altering active sites, by affecting regulatory sites, or by disrupting conformational stability and flexibility[3,4]. Mutations can also alter protein function through changes in protein-protein interactions[5–7] or subcellular localization[8,9]. Thus, the comprehensive characterization of the impact of a disease-associated missense mutation requires not only an analysis of the biochemical properties and known signaling activities of that protein, but also an unbiased assessment of its broader cellular properties, including its localization and interaction network.

Protein tyrosine phosphatases represent an important class of signaling proteins that are drivers of a variety of human diseases[10–15]. SHP2 is one such phosphatase with critical roles in cell signaling pathways[16–18], most notably an activating role of the Ras/MAPK pathway[19]. SHP2 has a catalytic protein tyrosine phosphatase (PTP) domain and two phosphotyrosine-recognizing SH2 domains that regulate its localization and activation (**Figure 1A**)[20]. The N-SH2 domain inhibits the PTP domain when not bound to phosphoproteins (**Figure 1B**), whereas the C-SH2 plays a minor role in auto-inhibition and primarily localizes SHP2 via phosphoprotein binding[21]. Dysregulation of SHP2 can lead to a variety of diseases with a wide range of phenotypes[22–27,17]. For example, mutations in SHP2 underlie a large fraction of cases of Noonan Syndrome (NS) and Noonan Syndrome with Multiple Lentigines (NSML), two similar but clinically distinct congenital disorders[28,29]. In addition, mutations in SHP2 are strongly associated with leukemias, most notably juvenile myelomonocytic leukemia (JMML), acute myeloid leukemia (AML), and acute lymphoblastic leukemia (ALL), and are occasionally also found in solid tumors[30,31].

Most well-characterized pathogenic SHP2 mutations are localized to the auto-inhibitory interface between the N-SH2 and PTP domains (**Figure 1C**). These mutations drive SHP2 hyperactivation by disrupting auto-inhibition. Mutations that disrupt SHP2 auto-inhibition can also alter protein-protein interactions, not only by allowing access the catalytic site, but also by putting the SH2 domains in a binding-competent state and exposing other cryptic binding interfaces[32–35] (**Figure 1D**). A significant number of clinically-observed mutations are located outside of the auto-inhibitory interface, many of which do not enhance basal catalytic activity[36]. Alternative hypotheses have been postulated for how some of these mutations cause diseases (**Figure 1E,F**)[7,37]. For example, the T42A mutation is in the N-SH2 ligand binding pocket, and studies have shown that this mutation can alter the affinity and specificity of the N-SH2 domain for phosphoproteins[7,38]. Furthermore, evidence has emerged that mutations in SHP2 can rewire its role in signaling networks by remodeling protein-protein interactions[7,39,40], underscoring the need for a broad and unbiased analysis of how SHP2 missense mutations alter SHP2 function.

Here, we profile the effects of missense mutations on the protein-protein interactions of SHP2, using proximity-labeling proteomics. We report the interactomes of wild-type SHP2 ($SHP2^{WT}$) and 10 disease-associated mutants, chosen for their diverse molecular and clinical effects. Our experiments identify mutation-specific changes in the SHP2 interaction network relative to $SHP2^{WT}$. Our results also pinpoint a role for SHP2 in the mitochondria, as well as enhanced mitochondrial localization and interactions for select mutants. We find that several SHP2 mutants with destabilized structures tend to localize more to the mitochondria, which can in turn affect mitochondrial homeostasis. We additionally map the remodeled interactome of SHP2 in the presence of the clinically-relevant allosteric inhibitor, TNO155, which stabilizes the auto-inhibited state. Our datasets expand the mechanistic paradigm for mutational effects in SHP2 and will be a resource for understanding SHP2 signaling and pathogenicity. Our work also illustrates a robust strategy for identifying mutation-driven effects on protein function using TurboID-proximity labeling.

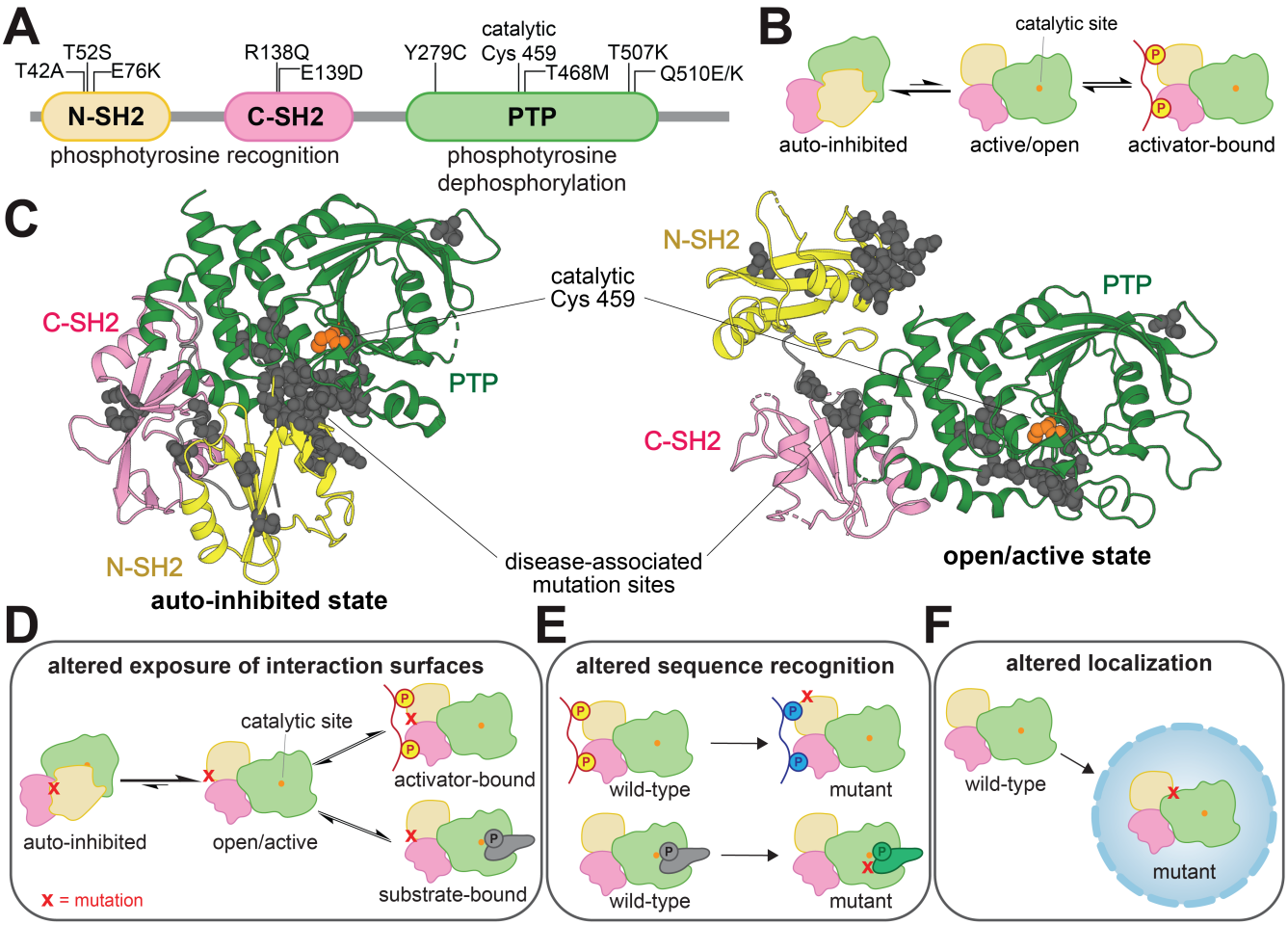

Figure 1. SHP2 regulation and dysregulation by mutations. (**A**) Domain architecture diagram of SHP2. Relevant mutations and the catalytic cysteine residue are labeled. (**B**) SHP2 is activated by the SH2 domains binding to phosphoproteins. (**C**) Visualization of common disease-associated mutations in SHP2 (gray spheres) in the auto-inhibited state (*left*, PDB: 4DGP) and open state (*right*, PDB: 6CRF). Cancer mutations cluster at the auto-inhibitory interface between the N-SH2 and PTP domains. Schematic diagrams showing that (**D**) mutations can alter the exposure of catalytic or non-catalytic interaction surfaces in SHP2, (**E**) mutations can alter sequence recognition in either the SH2 domain binding pockets or PTP domain active site, and (**F**) mutations can alter subcellular localization.

Results

Proximity-labeling proteomics identifies novel wild-type SHP2 interactors

The overarching goal of this study is to examine how mutations alter SHP2 protein-protein interactions, however we currently lack a dataset globally profiling $SHP2^{WT}$ interactions. Thus, we conducted affinity-purification mass spectrometry of overexpressed, myc-tagged $SHP2^{WT}$ from SHP2-knock-out HEK 293 cells to identify interacting proteins. Consistent with previous work[41], this experiment identified few interacting proteins, none of which were known SHP2 interactors (**Supplementary Figure 1A and Supplementary Table 1**). Furthermore, very few proteins co-immunopurified with $SHP2^{T42A}$, a mutant with enhanced binding affinity in the N-SH2 domain that would be expected to pull down more phosphoproteins (**Supplementary Figure 1B and Supplementary Table 1**). Signaling processes often require transient protein-protein interactions in order to be dynamic and reversible, and this feature may preclude facile identification of interactors by immunopurification[42]. Indeed, PTP domains are known to have weak and transient interactions with their substrates, making substrate identification by traditional immunopurification methods difficult[43]. Furthermore, SH2 domains generally have short-lived interactions with phosphoproteins, allowing for dephosphorylation of ligands by tyrosine phosphatases[44]. Given these innate features of signaling proteins, coupled with our low-yielding affinity purification mass spectrometry data, we reasoned that an alternative method was needed to map the SHP2 interactome.

To identify transient SHP2 interactions, co-localized proteins, and mutational differences, we implemented proximity-labeling proteomics using the engineered high-activity biotin ligase TurboID (**Figure 2A**)[45]. Previous studies have used the low-activity biotin ligase BirA to analyze or validate the interactomes of various tyrosine phosphatases[46–48], however, the data for SHP2 are sparse. We fused TurboID to the C-terminal tail of SHP2, given the important role the N-SH2 domain plays in SHP2 auto-inhibition. Using *in vitro* biochemical measurements, we confirmed that the resulting $SHP2^{WT}$-TurboID fusion protein retains catalytic activity and, like $SHP2^{WT}$, can be activated by SH2-domain engagement of phospho-peptides (**Supplementary Figure 2A**). We also confirmed that the hyperactivating E76K mutation, which disrupts autoinhibition, retains its effect in the context of a TurboID fusion (**Supplementary Figure 2B**). Furthermore, we ensured that SHP2-TurboID retains activity in cells and that this activity can be enhanced by the E76K mutation (**Supplementary Figure 2C-E**).

We next expressed $SHP2^{WT}$-TurboID and a TurboID-only control in SHP2 knock-out HEK 293 cells to profile the $SHP2^{WT}$ interactome[49]. In our experiments, SHP2-TurboID was expressed roughly 4-fold higher than the endogenous level in wild-type HEK 293 cells (**Supplementary Figure 2F**). Following established protocols, we isolated biotinylated proteins and identified them by mass spectrometry[50]. We identified 79 proteins with significant enrichment for $SHP2^{WT}$ over the TurboID-only control, applying a p-value cut-off of <0.05 and filtering for proteins with a $\log_2$ fold-change of >1 (**Figure 2B**, *top*, **and Supplementary Table 2**). Among the significantly enriched proteins were known SHP2 interactors, such as components of the Paf1 complex (Paf1, Ctr9, Leo1) and the scaffold protein Gab1 (**Figure 2B**, *top*)[51–54] We also observed enrichment of the mitochondrial peptidyl-prolyl isomerase PPIF, a protein previously shown to co-fractionate with SHP2, giving further confidence to the identified interactome[55].

In addition to known interactors, our proximity labeling revealed that SHP2 likely interacts or co-localizes with components of several functionally diverse protein complexes and pathways **(Supplementary Figure 3A and Supplementary Table 2)**. For example, we identified GDI1 and GDI2, which regulate the exchange of GDP and GTP in Rab proteins by inhibiting the dissociation of GDP, and UBL5 and SNRPE, components of the spliceosome. Previously, SNRNP27, another spliceosome component was identified as a putative interactor for SHP2[56]. We also observed proximity labeling of GBF1 and TMED2, which coordinate Golgi trafficking of COPI vesicles; as well as UPP1 and PNP, enzymes involved in pyrimidine and purine metabolism, respectively. Finally, we observed a distinctive strong signal for a number of mitochondrial proteins, including components of the electron transport chain, which we discuss extensively below. To ensure that these results truly represent increased protein-protein interactions or increased co-localization, as opposed to increased protein abundance, we also analyzed the total proteome of the matched cell lysates from which our TurboID experiments were performed. Proteins that were significantly enriched in the $SHP2^{WT}$-TurboID experiment, did not show

substantial changes in protein abundance (**Supplementary Figure 2G and Supplementary Table 3**), suggesting that SHP2-dependent enrichment in our proximity-labeling experiments is indeed due to interactions or co-localization, and not increased protein levels.

$SHP2^{WT}$ often engages in signaling by binding to phosphoproteins. Thus, we stimulated the epidermal growth factor receptor (EGFR), which phosphorylates many downstream proteins that bind to and activate SHP2[54]. We compared the interactome of $SHP2^{WT}$-TurboID to the TurboID control in cells stimulated with 100 ng/mL EGF and identified 32 proteins that were significantly enriched by $SHP2^{WT}$ (**Figure 2C**, *top*, **Supplementary Figure 3B, and Supplementary Table 2**). A few of these proteins, including Gab1 and components of the Paf1 complex, were also observed in unstimulated samples. However, most proteins were uniquely enriched in the EGF-stimulated samples. For example, we detected PI3KR2, a regulatory subunit of phosphatidylinositol-3 (PI3) kinase, which is a component of the EGF pathway and an established SHP2 interactor[57]. Critically, as done for the unstimulated sample, we confirmed that enriched proteins are not the result of increased protein abundance (**Supplementary Figure 2H and Supplementary Table 3**). We also directly compared $SHP2^{WT}$-TurboID with and without EGF stimulation to identify stimulation-dependent changes in the $SHP2^{WT}$ interactome. This comparison revealed 25 proteins with EGF-dependent enhanced proximity-labeling, including several components of the EGF pathway, along with proteins involved in transcription and RNA splicing (**Figure 2D**, *top*). Interestingly, 30 proteins had reduced biotinylation upon EGF stimulation, including PACSIN2 and SYNJ1, which are involved in the endocytosis of EGFR in absence of an EGF stimulus[58,59]. We also identified BIRC2, a modulator of mitogenic kinase signaling, and its interactor USP19[60,61], as well as checkpoint kinase ATM. Collectively, these experiments reveal the $SHP2^{WT}$ interactome, its restructuring by EGF stimulation, and several potentially novel functions for SHP2.

Protein tyrosine phosphorylation partly shapes the $SHP2^{WT}$ interactome

Given that all three globular domains of SHP2 can bind to tyrosine-phosphorylated proteins, we reasoned that a fraction of the SHP2 interactome should be dependent on tyrosine phosphorylation. Furthermore, we hypothesized that SHP2 interactions would be more driven by phosphotyrosine-containing proteins in the EGF-stimulated condition, given the overall increase in the abundance of phosphoproteins. We examined these hypotheses in two ways. First, using the PhosphoSitePlus database, we assessed what fraction of the proteins enriched in our TurboID dataset have potential tyrosine phosphorylation sites[62]. Proteins enriched by $SHP2^{WT}$-TurboID were more likely to have tyrosine phosphorylation sites than those enriched by the control (**Figure 2B,C***, bottom*). Furthermore, we found that the EGF-stimulated samples had a slight bias for proteins with tyrosine phosphorylation sites when compared with unstimulated samples (**Figure 2D***, bottom*). This analysis supports the idea that SHP2 interactions in our datasets are partly driven by tyrosine phosphorylation, and that interactions with tyrosine phosphorylated proteins increase upon EGF stimulation.

As an orthogonal evaluation of phosphotyrosine-dependent SHP2 interactions, we used the sequence specificities of the N- and C-SH2 domains to identify potential SH2 domain binding sites in our TurboID datasets. First, we conducted a high-throughput binding assay with the SHP2 N- and C-SH2 domains, using a degenerate ~10^6 peptide library containing a central phosphotyrosine and random flanking residues, as described previously (**Figure 2E and Supplementary Table 4**)[63]. These assays yielded position-specific weight matrices, which we used to score the ~40,000 tyrosine phosphorylation sites in the human proteome that are documented in the PhosphoSitePlus database (**Supplementary Table 4**)[62,63]. This scoring approach confidently identified several known SHP2 binding sites as high-affinity sequences (**Figure 2F**). In the proteins identified for $SHP2^{WT}$-TurboID in absence or presence of EGF stimulation, we identified 26 and 10 potential tyrosine phosphorylation sites, respectively, that are predicted to bind tightly to either the N-SH2 or C-SH2 domain of SHP2 (**Figure 2G**). These include phosphosites on known SHP2 binders, such as Gab1, Ctr9, and PI3KR2. They also include phosphosites on EXOC6, a member of the exocyst complex that has been connected to both EGFR and PI3 kinase signaling[64], and SH3BGRL proteins, which are adaptor proteins that can directly bind to EGFR-family kinases and modulate phosphotyrosine signaling[65]. This juxtaposition of biochemical and proteomic datasets provides additional mechanistic insights into specific SHP2 interactions.

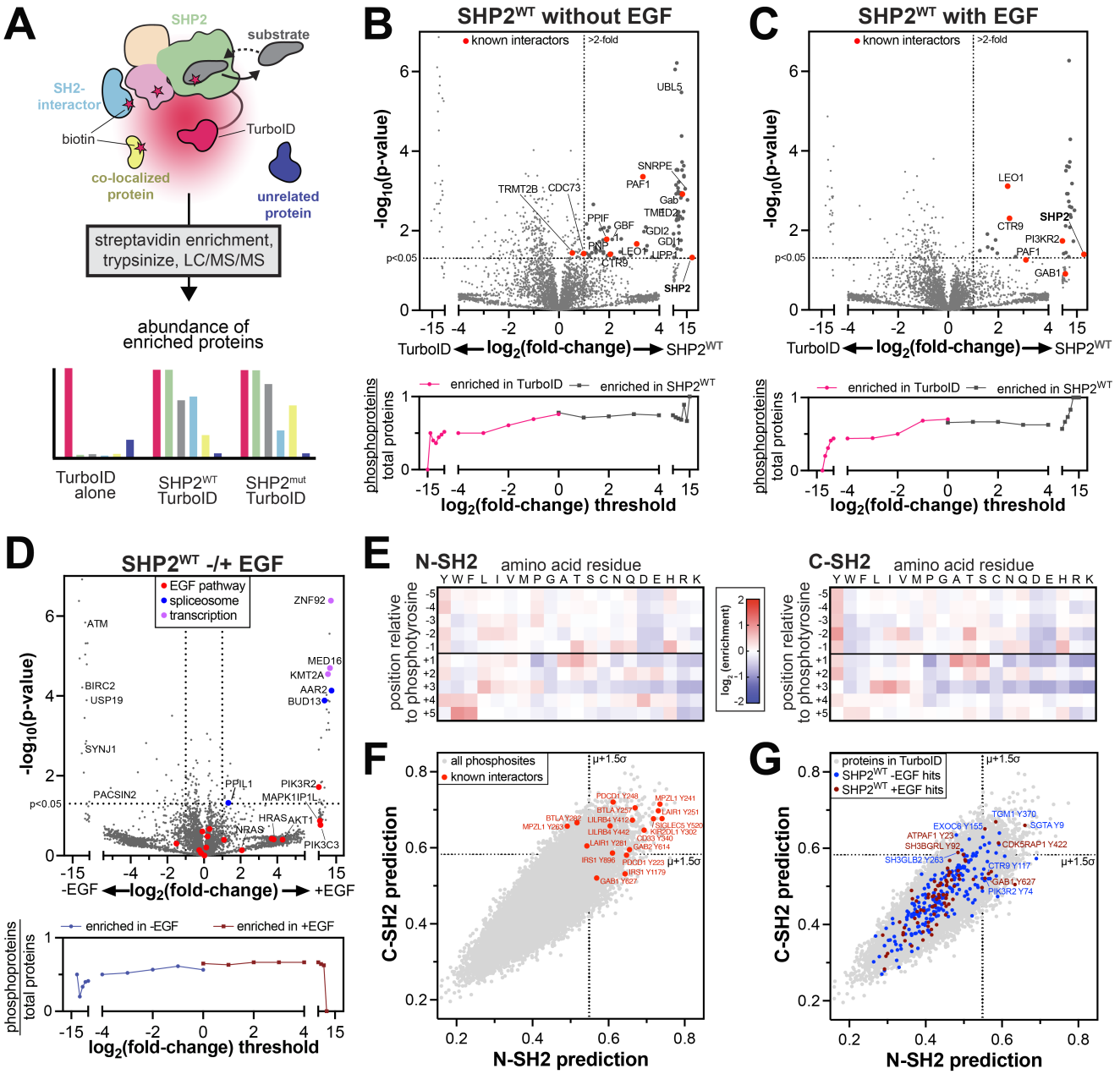

Figure 2. Profiling the interactomes of wild-type SHP2. (**A**) Schematic diagram of SHP2-TurboID experiments. TurboID generates reactive biotin derivatives, which label substrates, interactors, and co-localized proteins. MS/MS can be used to detect and quantify the interactome. (**B**) *top:* Comparison of SHP2^{WT}-TurboID with a TurboID-only control, in absence of EGF stimulation. Several known SHP2 interactors were identified, including proteins that are completely absent from the TurboID control. Gaps in the x-axis exclude non-significant points. Points at extreme x-values reflect proteins that were abundant in all SHP2-TurboID replicates and completely absent (imputed) in the TurboID-only control, or vice versa. *Bottom*: Analysis of the total number of potential phosphoproteins, as identified by PhosphoSitePlus, per total number of observed proteins above each fold-change threshold. (**C**) Same as (**B**) but with EGF stimulation. (**D**) *top*: Comparison of SHP2^{WT}-TurboID in unstimulated and EGF-stimulated conditions. Proteins involved in transcription, spliceosome, and the EGF pathway are indicated. *Bottom*: Analysis of the total number of potential phosphoproteins, as identified by PhosphoSitePlus, per total number of observed proteins above each fold-change threshold, for SHP2^{WT}-TurboID with and without EGF stimulation. (**E**) Heatmaps depicting position-specific weight matrices for peptide recognition by the SHP2 N-SH2 and C-SH2 domains. (**F**) Predicted scores for binding to the N-SH2 and C-SH2 domains for all phosphotyrosine sites in PhosphoSitePlus (gray dots). Phosphosites on several known interactors are labeled (red dots). (**G**) Predicted scores for binding to the N-SH2 and C-SH2 domains for all phosphosites on proteins in our proteomics dataset (gray dots). Phosphosites on proteins in the SHP2^{WT} interactomes are colored in blue (no EGF) and dark red (+EGF).

Pathogenic mutations have divergent effects on the SHP2 interactome

Having established a robust method to map the interactome of $SHP2^{WT}$, we then examined mutation-dependent changes in the SHP2 interactome. We compiled a panel of ten disease-associated SHP2 mutants, chosen for their distinct positions on the protein, varying effects on structure and activity, and diverse clinical outcomes (**Figure 3A**). Some of these mutants have been thoroughly characterized, predominantly via biochemical and biophysical experiments, whereas others remain more elusive. The Noonan Syndrome-associated T42A mutation enhances N-SH2 domain phosphoprotein binding affinity and specificity with a marginal effect on basal phosphatase activity[7,38,66]. By contrast, the nearby T52S mutation, which has been identified in JMML patients, does not substantially alter basal activity, ligand-binding affinity, or ligand-binding specificity[7], and its pathogenic mechanism is unknown. E76K is a well-studied JMML mutation found at the interface between the N-SH2 and PTP domains that disrupts auto-inhibition, yielding a constitutively active state of SHP2[67,68]. The melanoma mutant R138Q severely attenuates binding of the C-SH2 domain to phosphoproteins and might adopt a slightly more open protein conformation[7]. Curiously, the NS and JMML E139D mutation causes a substantial increase in activity despite not being at the auto-inhibitory interface, and reports of its effect on ligand-recognition by the C-SH2 domain have been conflicting[7,38]. Y279C and T468M, both located in the PTP domain and found in NSML, reduce the catalytic efficiency of SHP2 while destabilizing the auto-inhibited state[69]. T507K has been identified in solid tumors such as neuroblastoma and alters substrate specificity[40]. Finally, Q510K and Q510E both reduce catalytic activity[36], however Q510E has been identified in NSML and ALL, whereas Q510K has only been reported in patients with ALL. The interactomes and localization of most of these mutants have not been systematically explored.

We designed C-terminal TurboID fusions of all SHP2 variants, expressed these variants in SHP2 knock-out HEK 293 cells, and conducted proximity-labeling proteomics in the presence and absence of EGF stimulation. These datasets were compared to controls with just TurboID, and we defined the interactomes of each mutant using the same p-value (<0.05) and enrichment cut-off (>2-fold) used for $SHP2^{WT}$ (**Supplementary Table 2**). In the absence of EGF stimulation, the SHP2 mutants had between 13 and 39 overlapping hits with $SHP2^{WT}$, which showed enrichment for 79 proteins over the TurboID-control (**Supplementary Figure 4A**). In the presence of EGF, the interactome of each mutant was generally smaller (**Supplementary Figure 4B,C**). One plausible explanation for this is that, in unstimulated cells, SHP2 is more diffusely localized throughout the cell, whereas in EGF-stimulated cells membrane-proximal tyrosine kinase activity leads to recruitment of SHP2 to specific subcellular locations or recruitment sites. Given the overlap between SHP2 variants, we were able to identify a core SHP2 interactome, which we defined as proteins that are significantly enriched over the negative control for at least 4 out of the 11 SHP2 variants in unstimulated cells and 3 out of 11 variants with EGF stimulation, approximately 240 proteins in each case (**Figure 3B**). A gene ontology analysis on this core interactome revealed a conserved mitochondrial localization and interactions across SHP2 mutants (**Figure 3C,D and Supplementary Figure 5**). Both with and without EGF stimulation, these core SHP2 interactomes included mitochondrial ribosome proteins, but components of the respiratory chain complexes (e.g. NDUF and COX proteins) were distinctively enriched in the absence of EGF. By contrast, many cell cycle regulatory proteins were enriched in the EGF-stimulated core SHP2 interactome (e.g. CDK4 and CDC27), as was the EGFR-family kinase Her2 (ERBB2).

Despite the overlap between SHP2 variants, discussed above, we note that individual mutants displayed distinct interactomes from $SHP2^{WT}$ and from each other (**Supplementary Figures 4A,B and Supplementary Table 2**). While some of these differences are likely due to data sparsity or noise in our datasets, we hypothesize that many of these differences are due to changes in protein conformation or molecular recognition properties, as discussed in subsequent sections. Collectively, the analyses in this section show that pathogenic SHP2 mutants generally preserve some core functions of wild-type SHP2, but specific mutations partly remodel the SHP2 interactome, and this can be further altered by EGF stimulation.

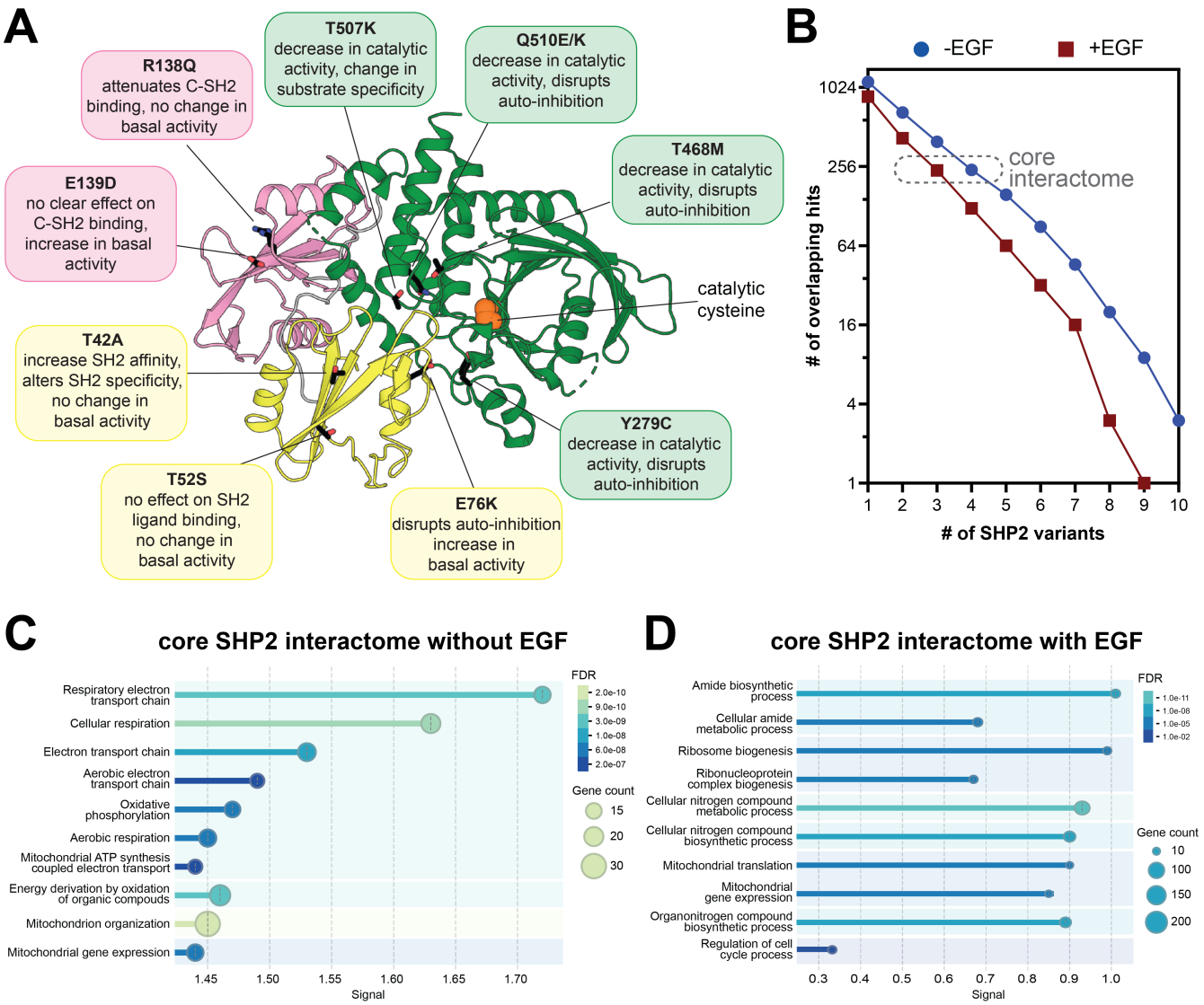

Figure 3. The interactomes of diverse pathogenic SHP2 variants. (**A**) Overview of mutations in this study. Their position on the auto-inhibited structure (PDB code 4DGP) are indicated, as are known characteristics of each mutant. (**B**) Number of overlapping proteins that are significantly enriched over the negative control for multiple SHP2 variants, both with and without EGF stimulation. (**C**) GO enrichment analysis for biological processes of the core SHP2 interactome without EGF stimulation. (**D**) GO enrichment analysis for biological processes of the core SHP2 interactome with EGF stimulation.

Mutation-dependent changes in phosphoprotein recognition underlie altered SHP2 interactomes

Given that many SHP2 interactions are driven by phosphoprotein binding, we first evaluated whether mutation-dependent changes in phosphoprotein recognition could underlie the remodeled interactomes. We focused our attention on the T42A and R138Q mutations in the N- and C-SH2 domains, respectively, which have distinct and dramatic effects on phosphoprotein binding (**Figure 3A**). We and others previously showed that the T42A mutation enhances the affinity and alters specificity of the N-SH2 domain for phosphoproteins[7,38]. Consistent with this, in our proximity-labeling datasets, we observed an overall increase in the number of proteins enriched by $SHP2^{T42A}$ over $SHP2^{WT}$ (**Figure 4A and Supplementary Figure 4A-C**). Several proteins with known tyrosine phosphorylation sites were enriched by $SHP2^{T42A}$ over $SHP2^{WT}$, including MPZL1 and ACOX1 (**Figure 4B**). In our previous work using proteome-derived phospho-peptide libraries to profile SHP2 SH2 mutants, we found that phosphosites on these proteins showed enhanced binding to $N\text{-}SH2^{T42A}$ with respect to $N\text{-}SH2^{WT}$, providing a mechanistic explanation for the enrichment of these proteins in our $SHP2^{T42A}$ interactome (**Figure 4C**)[7].

Notably, MPZL1 has previously been shown to interact with SHP2, and enhancement of this interaction through SHP2 NSML mutations is linked to hypertrophic cardiomyopathy[34]. Unlike $SHP2^{T42A}$, a Noonan Syndrome mutant, NSML mutants like $SHP2^{T468M}$ and $SHP2^{Q510E}$ have a higher propensity to adopt the open conformation, allowing them to more readily bind phosphoproteins, but these mutants generally also have impaired catalytic activity[37]. MPZL1 has been shown to be hyperphosphorylated on Y241 and Y263 in NSML, due to the enhanced protective effect of SHP2 SH2 domains on the phosphorylated tyrosines conferred by the open-conformation-inducing mutations[70]. Indeed, like $SHP2^{T42A}$, the NSML $SHP2^{T468M}$, $SHP2^{T507K}$, and $SHP2^{Q510E}$ mutants showed increased interaction with MPZL1 in our TurboID data relative to $SHP2^{WT}$ (**Supplementary Figure 4D**). We further validated the enrichment of MPZL1 by $SHP2^{T42A}$ by co-immunopurification, which showed that the T42A mutation both enhances MPZL1 binding and shows increased in MPZL1 phosphorylation (**Figure 4D**). This demonstrates that $SHP2^{T42A}$, despite not adopting a more open conformation than $SHP2^{WT}$, converges on increased interaction with MPZL1 through altered sequence-recognition in the N-SH2 domain[7].

The R138Q mutation in the C-SH2 domain removes a conserved Arg residue in SH2 domains that is required for tight phosphotyrosine binding, and we previously showed that this mutation severely weakens phosphopeptide binding to the C-SH2 domain[7]. Surprisingly, in our TurboID proximity-labeling experiments we observed more proteins enriched with $SHP2^{R138Q}$ than $SHP2^{WT}$, suggestive of increased interactions or increased co-localization with other proteins (**Figure 4E,F,** *top***, and Supplementary Figure 4A-C**). Since this mutation disrupts C-SH2-phosphoprotein interactions, we suspected that proximity-labeling with $SHP2^{R138Q}$ would be less dependent on tyrosine phosphorylation than with $SHP2^{WT}$. Indeed, proteins enriched by $SHP2^{R138Q}$ are less likely to be phosphoproteins than those enriched by $SHP2^{WT}$ (**Figure 4E,F,** *bottom*)[62]. Given that the C-SH2 domain of SHP2 is critical for localization, one plausible explanation for the anomalous increase in proximity labeling with $SHP2^{R138Q}$ is that the loss of C-SH2 function leads to SHP2 mislocalization and promiscuous protein-protein interactions. Overall, our representative analyses of $SHP2^{R138Q}$ and $SHP2^{T42A}$ reveal how changes in phosphoprotein recognition can measurably alter the interactome of a signaling protein.

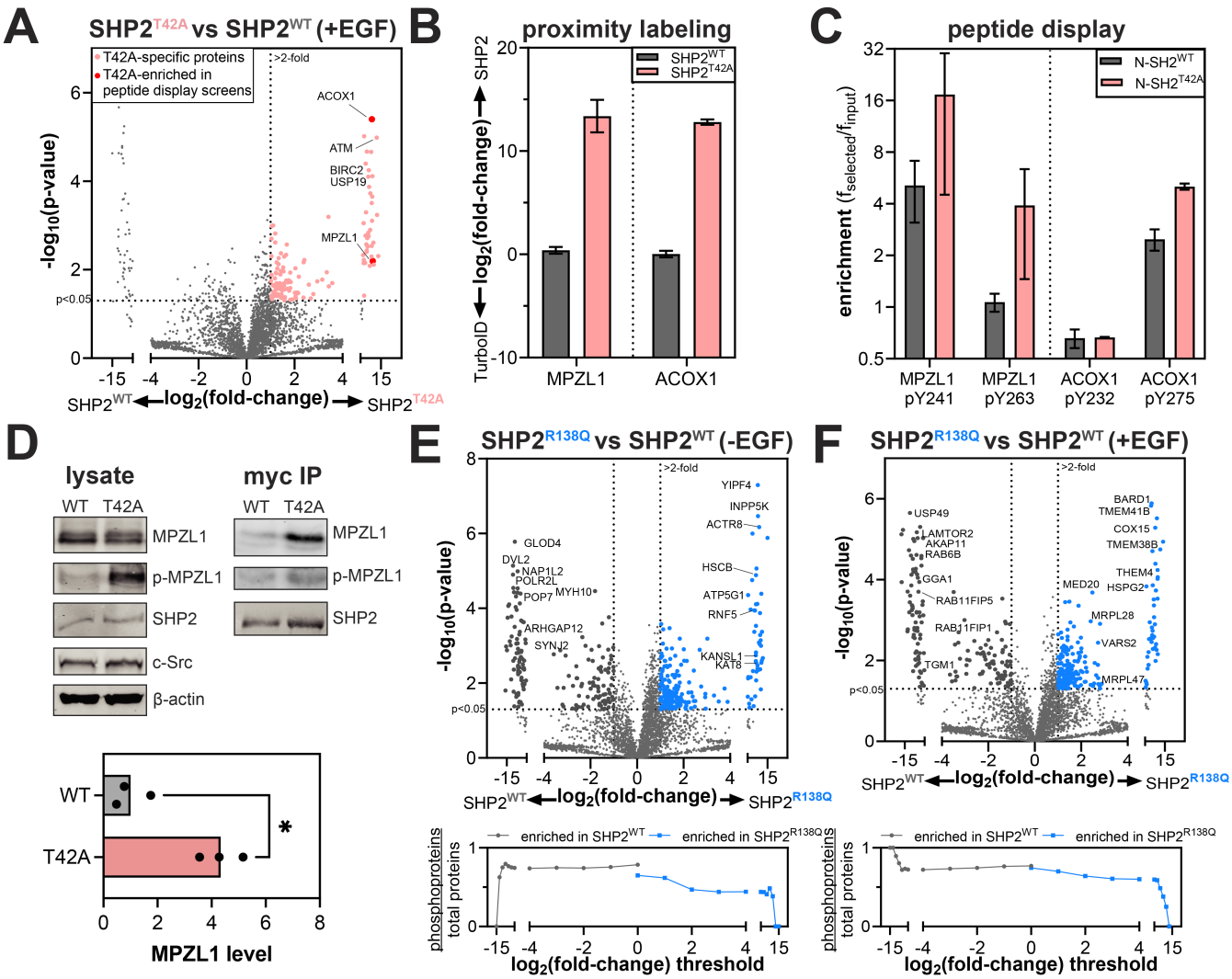

Figure 4. Rewired interactomes in SHP2 mutants with altered phosphoprotein binding properties. (**A**) Volcano plot showing enriched proteins in SHP2^{T42A}, compared to SHP2^{WT}. (**B**) Log_2 fold-change in enrichment for MPZL1 and ACOX1 by SHP2^{WT} and SHP2^{T42A} compared with the TurboID control. (**C**) Enrichment of MPZL1- and ACOX1-derived phosphopeptides from peptide display screens using the SHP2 N-SH2^{WT} and N-SH2^{T42A} domains. (**D**) Phosphorylation levels and co-immunopurification of MPZL1 by SHP2^{WT} and SHP2^{T42A}. Quantified MPZL1 levels in the myc-SHP2 co-IP are shown in the graph. Asterisk denotes p<0.05. (**E**) (*top*) Volcano plots highlighting enriched proteins in SHP2^{R138Q}, compared to SHP2^{WT} in the absence of EGF stimulation. (*bottom)* Analysis of the total number of potential phosphoproteins, as identified by PhosphoSitePlus, per total number of observed proteins past each fold-change threshold for SHP2^{WT} versus SHP2^{R138Q}. The SHP2^{R138Q} interactome is less enriched in potentially tyrosine-phosphorylated proteins than the SHP2^{WT} interactome. No negative selection against tyrosine phosphorylation sites is observed for SHP2^{WT}. (**F**) Same as (**E**), but with EGF stimulation.

Pathogenic mutations remodel the SHP2 mitochondrial interactome

As noted above, mitochondrial proteins make up a large component of the core SHP2 interactome in our datasets (**Figure 3C,D and Supplementary Figure 5**). For example, $SHP2^{WT}$ showed enrichment of 21 mitochondrial proteins over the TurboID-only control in the absence of EGF stimulation (**Figure 5A**). This is consistent with previous work demonstrating that SHP2 can localize to mitochondria[71–77]. As further validation, we analyzed endogenous SHP2 localization by fluorescence microscopy, which confirmed that SHP2 can indeed localize to the mitochondria (**Supplementary Figure 6A**). Levels of biotin in the mitochondria can differ from that in the cytoplasm or other organelles, which could bias subcellular TurboID signal[78–80]. To check for this, we conducted TurboID experiments both with and without addition of exogenous biotin to the cells. We found that there was no bias in mitochondrial biotinylation coming from basal biotin levels, and that the enhanced biotinylation signal in our experiments depends on the addition of exogenous biotin (**Supplementary Figure 6B**). Furthermore, this effect was stronger in unstimulated cells when compared with EGF-stimulated cells, suggesting that the mitochondrial localization of SHP2 is dependent on its signaling state (**Supplementary Figure 6B**).

Although every SHP2 variant showed proximity labeling of mitochondrial proteins, we noticed a distinctive increase in mitochondrial signal for R138Q, T468M, Q510K, and to a lesser extent, E76K (**Figure 5B and Supplementary Figure 7**). To validate this effect, we expressed several mutants without TurboID fusion in SHP2 knock-out HEK 293 cells, isolated mitochondria, and blotted for SHP2 (**Figure 5C**). We also analyzed a control mutant, $SHP2^{R4A+R5A}$, which has a defective mitochondrial localization signal[75]. These experiments confirmed that some SHP2 mutants have more mitochondrial localization than $SHP2^{WT}$ (**Figure 5C**). SHP2 mutations can cause Noonan Syndrome and cardiomyopathy, with symptoms that resemble those in primary mitochondrial disorders[81]. Furthermore, disease-associated activating SHP2 mutants have been shown to impact mitochondrial function and homeostasis[77,82]. Thus, the increased mitochondrial localization for some mutants could contribute to pathogenicity, warranting a deeper analysis of the specific interactions and functions of SHP2 in this organelle.

SHP2 has been reported to interact with proteins in complex I and III of the electron transport chain, and SHP2 mutations can modulate mitochondrial respiration[77,83]. Consistent with this, our data show that many SHP2 variants have enhanced proximity labeling of electron transport chain proteins relative to the TurboID control (**Figure 5D**). $SHP2^{WT}$ primarily labeled components of complex I and complex IV. Many mutants also labeled complexes I and IV, however we observed mutant-specific changes in proximity to various components of the electron transport chain. For example, whereas $SHP2^{WT}$ only labeled accessory subunits of complex I, $SHP2^{T468M}$ also labeled assembly- and core-subunits, suggestive of a longer residency near complex I. Notably, we saw no labeling of complex III by $SHP2^{WT}$, and this was recapitulated in most SHP2 mutants. By contrast, several mutants showed an increase in labeling of complex V proteins (**Figure 5D**). These data suggest that SHP2 mutants could potentially alter core mitochondrial functions, such as oxidative phosphorylation. Indeed, we found that a few SHP2 mutants, particularly $SHP2^{T468M}$, could enhance the formation of mitochondrial reactive oxygen species, suggesting that SHP2 mutants differentially alter mitochondrial energy production (**Figure 5E**).

Finally, we sought to identify new binding sites for SHP2 in the mitochondria that could inform future functional investigations. There are 165 proteins that are enriched for at least three SHP2 variants (either with or without EGF stimulation). We scored the 400 putative tyrosine phosphorylation sites on these proteins for their binding propensity to either N-SH2 or C-SH2 domain, as described above (**Figure 2E-G**)[63]. Among these, we found phosphosites on NDUFA5, UQCRQ, and NDUFA4, components of complex I, III, and IV of the electron transport chain, respectively (**Figure 5F and Supplementary Table 4**). We also identified a high-scoring phosphosite on ATPAF1, an assembly factor of the F(1) component of ATP synthase, which SHP2 has not previously been reported to bind to. We validated that SHP2 can directly interact with ATPAF1 via co-immunopurification (**Figure 5G**). Previously, SHP2 has also been shown to directly bind to NDUFB8[77], which did not pass the significance threshold in our TurboID experiments but has a high-scoring phosphosite for both domains. Finally, we note that some potential binding sites were on proteins that were selectively observed in SHP2 mutant interactomes but not the $SHP2^{WT}$ dataset. These include some members of respiratory complexes, as seen above, as well as Hsp40-family co-chaperones SACS (sacsin) and DNAJA3, which we discuss in the next section. Our

interactomics data spanning multiple complexes of the electron transport chain expand the scope SHP2 interactors in the mitochondria and suggest plausible roles in this subcellular compartment.

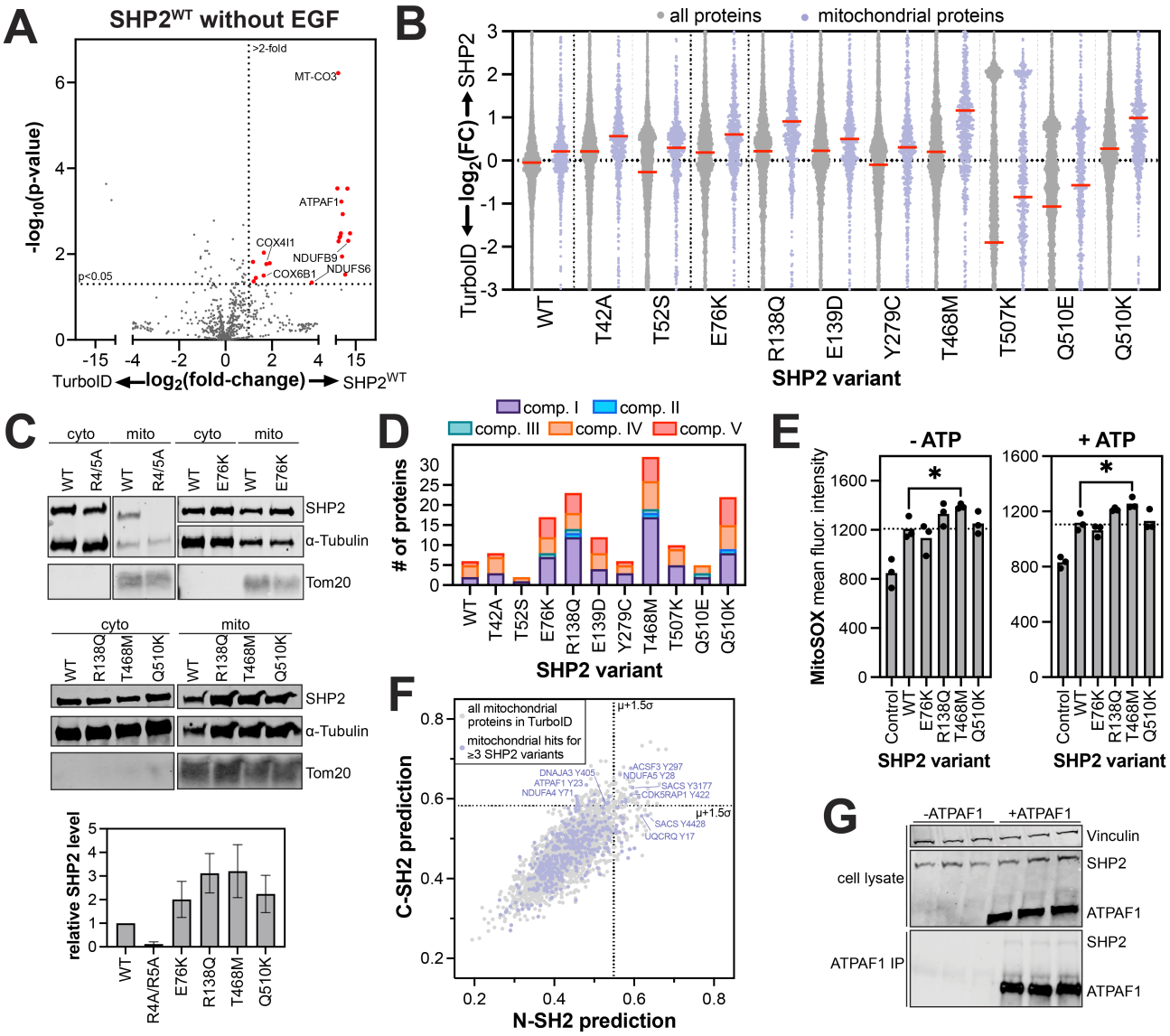

Figure 5. SHP2 interactions in the mitochondria. (**A**) Volcano plot of the mitochondrial proteins in our TurboID dataset, showing many mitochondrial proteins that are significantly enriched by SHP2^{WT}-TurboID compared to the TurboID-only control, in absence of EGF stimulation. (**B**) Enhanced proximity labeling of mitochondrial proteins by SHP2 variants relative to the TurboID-only control (lilac), compared to proximity labeling of the whole proteome (gray). (**C**) Cellular fractionation and western blots confirming enhanced mitochondrial localization of SHP2^{E76K}, SHP2^{R138Q}, SHP2^{T468M}, and SHP2^{Q510K}, relative to SHP2^{WT}. SHP2$^{R4A/R5A}$, with a defective mitochondrial localization signal, shows reduced mitochondrial abundance. (**D**) The number of electron transport chain proteins significantly enriched over TurboID for each SHP2 variant in the absence of EGF stimulation. (**E**) MitoSOX staining showing increased reactive oxygen species for SHP2^{T468M} (-/+ ATP). (**F**) N-SH2 and C-SH2 predictions for human phosphosites. Select high-scoring mitochondrial phosphosites are labeled. (**G**) Co-immunopurification of SHP2^{WT} by ATPAF1, co-expressed in HEK293 cells. Three independent replicates are shown on the same blots.

Destabilization of SHP2 protein structure might contribute to mitochondrial import

We identified several SHP2 mutants which localize more to the mitochondria than the wild-type protein, but the mechanism by which this happens is unclear. The Tom40 import channel complex has been shown to be critical for the translocation of SHP2 through the outer mitochondrial membrane[75]. Indeed, we found that $SHP2^{WT}$ and most mutants proximity-labeled Tom40 more than the TurboID control (**Figure 6A**), however there did not appear to be mutant-specific enhanced engagement of this core component of the import channel. Tom20, a component of the Tom40 complex, binds mitochondrial localization sequences on cytoplasmic proteins, often at their N-termini[84], and SHP2 has a reported mitochondrial localization motif near its N-terminus (R4 to H8)[75]. Mutation of Arg4 and Arg5 to alanine residues diminishes mitochondrial localization (**Figure 5C**)[75]. Notably, Tom20 is an enriched protein for several SHP2 mutants but not $SHP2^{WT}$, as are other secondary components of the Tom20/Tom40 complex (**Figure 6B and Supplementary Figure 8A**). Furthermore, in a recent Tom20 proximity-labeling study, SHP2 was identified as a proximal protein[85]. We hypothesized that some SHP2 mutants might have enhanced mitochondrial localization due to conformation-dependent changes in the accessibility of the localization signal (**Figure 6C**). We analyzed our previously-reported molecular dynamics simulations of SHP2 in both the auto-inhibited state and an open state that is likely accessed by some disease mutants. These simulations showed a modest increase in solvent accessibility for R4 and F7 in the open conformation, but not for R5 (**Figure 6D**)[36]. Based on this analysis, it is plausible but not conclusive that SHP2 mutations alter Tom20 access to the mitochondrial localization sequence.

SHP2 has been observed both in the intermembrane space and the mitochondrial matrix, but most reported functions are in the matrix[71,75,77,83]. We conducted a deeper analysis of submitochondrial localization in our proteomics datasets and found that $SHP2^{WT}$ has disproportionately more labeling of intermembrane space proteins than the mutants with increased mitochondrial signal (**Figure 6E**). This suggests that there is accumulation of $SHP2^{WT}$ in the intermembrane space or more efficient transport of some mutants through the inner mitochondrial membrane. Transport of soluble proteins through the inner membrane is typically mediated by the Tim23 complex. While components of this complex are present in our datasets, most do not show strong signal, other than Tim17B (**Supplementary Figure 8B**).

Transport through both mitochondrial membranes and protein maturation in the mitochondrial matrix are highly dependent on chaperone proteins, most notably the Hsp70/40 system[86]. SHP2 is a known Hsp70 client[87], however, neither cytoplasmic Hsp70 (HSPA1A/HSPA1B), nor its mitochondrial counterpart mortalin (HSPA9) were statistically significant hits for any SHP2 variant in our TurboID datasets (**Supplementary Figure 8C**). However, we did observe distinctive SHP2-specific signal for multiple Hsp40/DnaJ proteins, most notably DnaJA3, DnaJC11, and DnaJC19, all of which play critical roles in the mitochondria[88]. For these three mitochondrial Hsp40/DnaJ proteins, we observed enhanced TurboID signal for several SHP2 mutants relative to $SHP2^{WT}$, suggesting that the mutants have enhanced association with Hsp40 in the mitochondria (**Figure 6F**). DnaJC19 is thought to play a role in facilitating protein translocation through the inner mitochondrial membrane in coordination with Tim23[89], DnaJA3 is critical for mitochondrial matrix proteostasis[90], and DnaJC11 is involved in cristae formation and import of mitochondrial proteins[91]. It is noteworthy that, like SHP2, these proteins have been connected to significant developmental disorders and cardiomyopathies[92,93]. These observations suggest that interactions with Hsp40 proteins could modulate the mitochondrial activity of SHP2 mutants.

SHP2 likely interacts with Hsp40/DnaJ proteins to facilitate its unfolding and refolding as it traverses the mitochondrial membranes. These interactions presumably depend on the stability of the SHP2 variant. The auto-inhibited state of SHP2 is compact and defined by extensive interdomain interactions, most likely making it more thermally stable than the SHP2 open state. Consistent with this, SHP2 mutants that adopt a more open conformation tend to have lower melting temperatures by differential scanning fluorimetry[7,36,94,95]. We previously showed that $SHP2^{R138Q}$ and $SHP2^{T468M}$ have lower melting temperatures than $SHP2^{WT}$ and show here that $SHP2^{Q510K}$ also has a decreased melting temperature (**Figure 6G**)[7,36], suggesting that these mutants have a destabilized auto-inhibited state and/or decreased overall thermal stability. Collectively, our proximity labeling data and stability measurements paint a plausible picture for mutation-dependent SHP2 translocation to the mitochondrial matrix, dictated by changes in protein stability and association with mitochondrial chaperones.

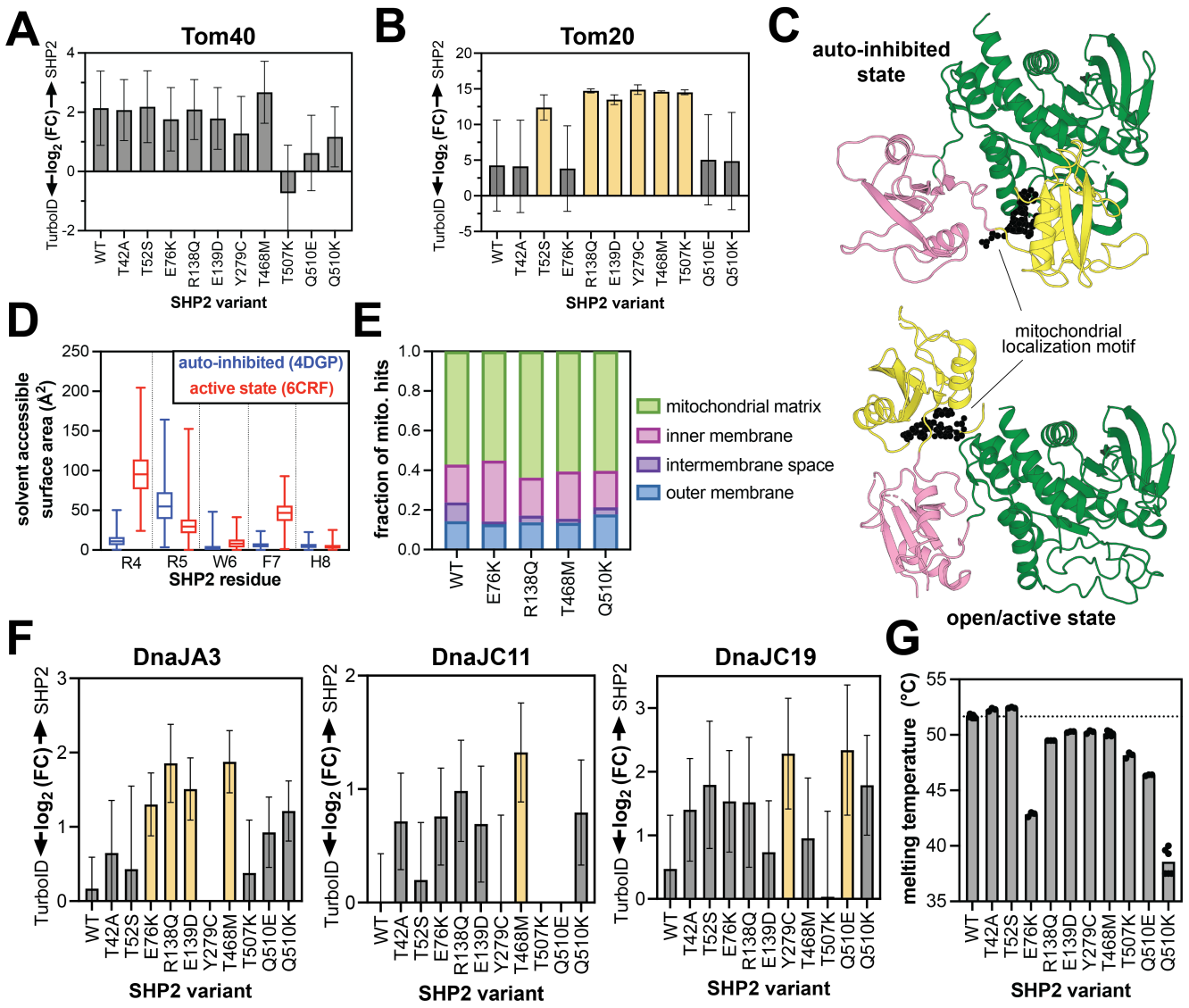

Figure 6. Protein interactions and structural features impacting SHP2 mitochondrial import. Proximity-labeling of (**A**) Tom40 and (**B**) Tom20 outer mitochondrial import machinery. Variants in yellow are significantly enriched over the TurboID control (fold-change >2, p-value <0.05). (**C**) The SHP2 mitochondrial localization motif (R4 to H8) highlighted as black spheres on auto-inhibited (*left*, PDB code 4DGP) and open (*right*, PDB code 6CRF) structures. (**D**) Differences in solvent accessibility of the RRWFH motif in molecular dynamics simulations using auto-inhibited conformation (starting structure PDB code 4DGP) or open conformation (starting structure PDB code 6CRF). (**E**) Sub-mitochondrial localization of SHP2 variants inferred from proximity-labeling patterns. (**F**) Proximity-labeling signal for mitochondrial Hsp40/DnaJ proteins, DnaJA3, DnaJC11, and DnaJC19. Variants in yellow are significantly enriched over the TurboID control (fold-change >2, p-value <0.05). (**G**) Melting temperatures of SHP2 variants measured by differential scanning fluorimetry.

Allosteric inhibition remodels the SHP2 interactome by stabilizing the auto-inhibited state

Our results thus far illustrate how changes to the conformation and stability of SHP2 can have profound effects on its interactome and localization. Over the past decade, several allosteric inhibitors of SHP2 have entered clinical trials for cancer treatment, and many of these molecules bind in a "tunnel" site between the C-SH2 and PTP domains to stabilize the auto-inhibited state (**Figure 7A**)[96,97]. TNO155, also known as batoprotafib, binds to this tunnel site and is one of the more potent SHP2 inhibitors[98]. Given its effect on SHP2 conformation and stability, we examined how TNO155 alters the SHP2 interactome. We pre-incubated $SHP2^{WT}$-TurboID-transfected cells for 4 hours with 1 μM TNO155 then conducted proximity-labeling proteomics experiments. Direct comparison of $SHP2^{WT}$ and $SHP2^{WT+TNO155}$ datasets revealed that inhibitor treatment dramatically reduced the number of interactors (**Figure 7B,C**). In unstimulated cells, 210 proteins were significantly enriched in inhibitor-treated samples over untreated samples, whereas 480 proteins were significantly enriched in untreated samples over inhibitor-treated ones (**Supplementary Table 2**). In presence of EGF, we also observed a large number of proteins enriched in untreated cells over TNO155-treated cells. These results are consistent with the auto-inhibited state of SHP2 being less capable of engaging in protein-protein interactions.

Given that TNO155 and other allosteric SHP2 inhibitors enforce the auto-inhibited state, we hypothesized that inhibitor binding would enhance the overall thermal stability of SHP2, which in turn could impact SHP2 mitochondrial import. We first measured the melting temperatures of $SHP2^{WT}$ and several mutants with enhanced mitochondrial localization in the absence and presence of TNO155 (**Figure 7D**). Each SHP2 variant showed an increase in melting temperature upon addition of TNO155, albeit to varying extents. This variability likely reflects the extent to which SHP2 adopts an open conformation that lacks the inhibitor binding site. Indeed, $SHP2^{E76K}$ showed the smallest increase of ~2 °C, which is consistent with this mutant almost exclusively inhabiting the open conformation, which lacks the inhibitor binding pocket[67,99]. By contrast, $SHP2^{Q510K}$ showed a dramatic increase of 13 °C, but the molecular basis for this effect is not immediately obvious. Regardless, these results show that TNO155 binding can enhance the stability of SHP2.

Next, we examined the specific mitochondrial signal in $SHP2^{WT}$-TurboID experiments with and without TNO155. For $SHP2^{WT}$ in unstimulated cells, as discussed in earlier sections, we identified 78 proteins with significant enrichment over the TurboID-only control (>2-fold, p-value <0.05), 21 of which were proteins with a known mitochondrial localization (**Figure 5A**). 13 of these mitochondrial proteins were no longer significantly enriched over the TurboID-only control upon addition of TNO155 (**Figure 7E,** *left*), supporting the notion that SHP2 stability is a driving factor in its subcellular localization. Remarkably, a few mitochondrial $SHP2^{WT}$ interactors were still enriched upon TNO155 treatment (**Figure 7E,** *right*). These proteins could be interactors that engage SHP2 via interfaces that are not impacted by inhibitor binding, or they may be co-localized proteins that are not dependent on SHP2 conformation. Alternatively, these proteins might bind tightly to SHP2 in the open state, rendering it insensitive to TNO155. Indeed, previous studies have shown that phosphoprotein binding desensitizes SHP2 to allosteric inhibition[68]. Notably, both NDUFB9 and ATPAF1 have predicted high-affinity N- or C-SH2 binding sites (**Supplementary Table 4**). Critically, these different mechanisms warrant further investigation, as they could have implications for inhibitor efficacy. Collectively, the results in this section show that the allosteric inhibitor TNO155 can alter both SHP2 interactions and localization by changing its overall conformation and stability. These results also highlight the exquisite sensitivity and broad applicability of TurboID proximity labeling to examine state-dependent changes in SHP2 function.

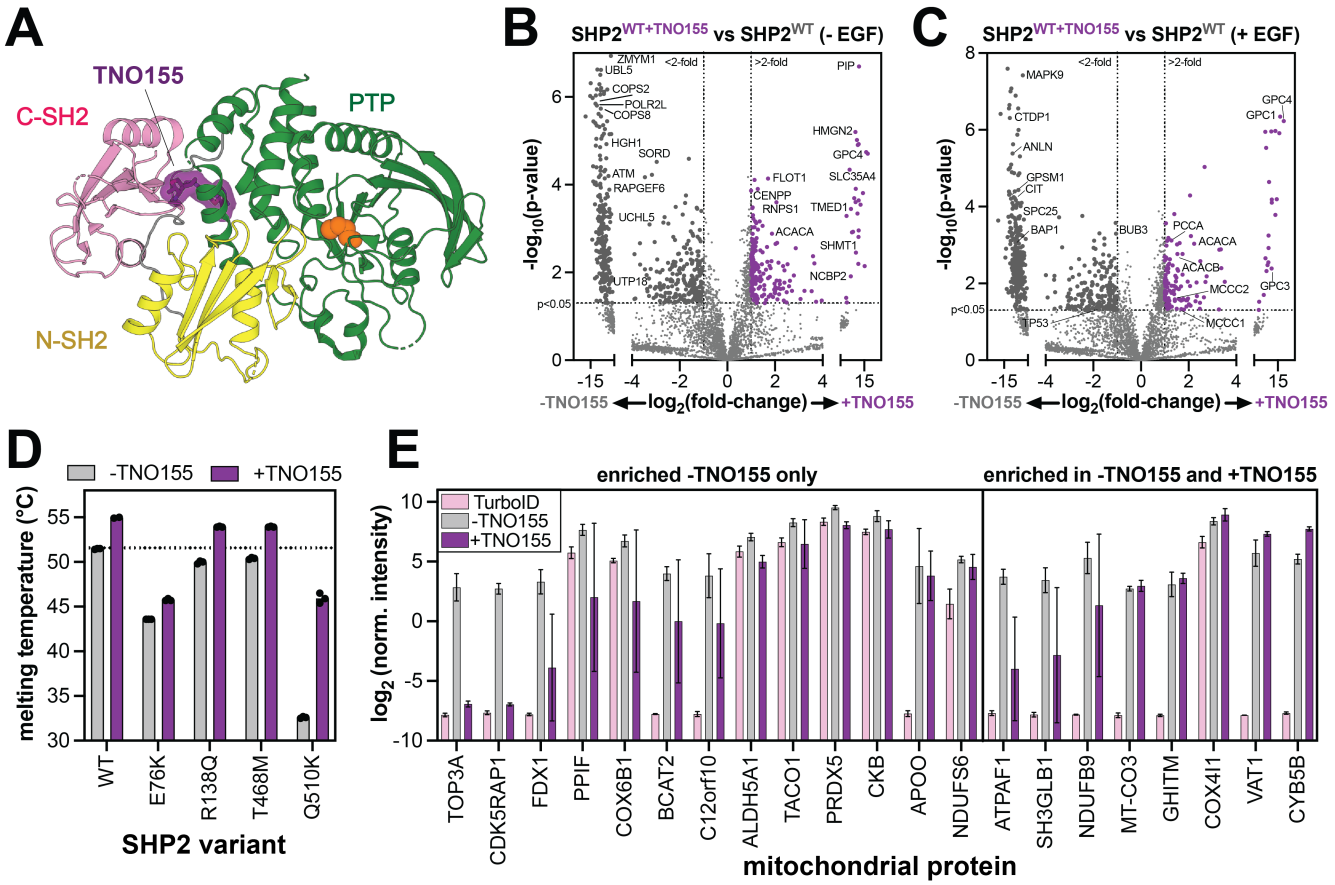

Figure 7. Alteration of SHP2 interactions by the allosteric inhibitor TNO155. (**A**) Structure of SHP2 with allosteric inhibitor TNO155 docked in the tunnel site between the C-SH2 domain and the PTP domain (PDB: 7JVM). (**B**) Volcano plot highlighting enriched proteins in $SHP2^{WT}$, compared to $SHP2^{WT+TNO155}$ in the absence of EGF stimulation. (**C**) Volcano plot highlighting enriched proteins in $SHP2^{WT}$, compared to $SHP2^{WT+TNO155}$ in the presence of EGF stimulation. (**D**) Melting temperatures of SHP2 variants measured by differential scanning fluorimetry in absence and presence of 10 μM TNO155. (**E**) Normalized intensities for 21 mitochondrial proteins that are significantly enriched in $SHP2^{WT}$ versus TurboID-only. Intensities are shown for the TurboID-only control (pink), $SHP2^{WT}$ without TNO155 (gray), and $SHP2^{WT}$ with TNO155 (purple). The 13 proteins on the left are not significantly enriched in the +TNO155 sample over the TurboID-only control. The 8 proteins on the right are significantly enriched in the +TNO155 sample over the TurboID control.

Discussion

The role of SHP2 in cancer and congenital disease is well-established. Disease-driving mutations in *PTPN11,* the gene encoding SHP2, are almost exclusively missense mutations[24]. Many canonical mutations, which disrupt the auto-inhibitory interface and hyperactivate SHP2, have been thoroughly characterized. This work has broadened our understanding of the protein-intrinsic regulation of SHP2 and shed light on how dysregulation of SHP2 can cause disease. While SHP2 is known to function in a large variety of cell signaling pathways, its role in disease has largely been linked to dysregulation of the Ras/MAPK pathway[18,19,100–102]. Recent studies have started to show the diverse effects that mutations in SHP2 can have on the protein itself and its function in cellular context. For example, some catalytically inactive NSML mutants can still drive proliferative signaling through increased adoption of an open conformation, which enhances SH2-phosphoprotein interactions[37,103]. Additionally, some mutations can alter substrate- or ligand-binding preferences and rewire signaling interactions[7,40]. This diversity of potential mutational effects led us to probe the cellular interactomes of diverse SHP2 mutations using proximity-labeling proteomics. We hypothesized that mutations could alter the protein interaction network of SHP2, and mapping these remodeled interactomes could provide insights into aberrant cell signaling.

The results presented in this study show that proximity-labeling proteomics by TurboID allows for in-depth comparison of mutation- and drug-induced conformational changes to SHP2, as well as its effect on the protein-protein interactions and localization. We mapped the interactomes of SHP2^{WT} and 10 SHP2 mutants, chosen for their diversity of molecular, cellular, and clinical effects. We found that individual SHP2 mutants have overlapping but also partly distinct interactomes, which reveal both divergent and convergent modes of dysregulation. For example, the melanoma mutant SHP2^{R138Q} has a dysfunctional C-SH2 domain, and interactions with this mutant appear to be less dependent on protein phosphorylation, suggesting critical alternative modes of protein-protein engagement for SHP2. The Noonan Syndrome mutant SHP2^{T42A} enhances intrinsic phosphoprotein binding affinity and alters binding specificity, causing it to have a tighter interaction with the cell surface receptor MPZL1. SHP2^{T42A} biochemically phenocopies NSML mutants SHP2^{T468M}, SHP2^{T507K}, and SHP2^{Q510E}, which adopt an open conformation that also stabilizes their interaction with MPZL1. This observation highlights how mechanistically distinct mutations can yield similar cellular and clinical phenotypes.

Another highlight of our study is the juxtaposition of SHP2 proximity-labeling data with predictions of SH2 binding sites across the proteome. This analysis revealed a number of tyrosine phosphorylation sites that could recruit and directly modulate SHP2 function. The PTP domain of SHP2 also interacts with phosphosites, to dephosphorylate them. One limitation of our work is that we cannot differentiate binders and co-localized proteins from direct substrates using proximity-labeling proteomics alone, and the SHP2 PTP domain likely does not have strong sequence preferences that could be used to predict substrates[49]. One possibility would be to combine substrate-trapping mutations with proximity-labeling, to selectively enhance signal for substrates over other proximal proteins, as done recently for another phosphatase[104]. However, we caution that for SHP2, some substrate-trapping mutations, most notably C459S, cause dramatic structural rearrangements that will have collateral effects on SHP2 localization and the measured interactome[67,105]. Thus, careful assessment of the structural effects of substrate-trapping mutants will be required.

A notable feature of our proximity-labeling datasets was that we observed a strong mitochondrial signal for SHP2^{WT} and several mutants. The role of SHP2 in mitochondria is not well-understood. Studies have shown involvement of SHP2 in the inflammasome through interaction with ANT1 and demonstrated that SHP2^{E76K} can enhance mitochondrial metabolism through excessive dephosphorylation of STAT3[75,77]. Hyperactive SHP2 variants have also been reported to dysregulate mitochondrial metabolism, causing oxidative stress in cells[39,74,83]. Here, we show that several SHP2 variants co-localize with components of the electron transport chain. Furthermore, we show that SHP2^{R138Q}, SHP2^{T468M} and SHP2^{Q510K}, and to lesser extent SHP2^{E76K}, have increased mitochondrial localization relative to SHP2^{WT} and some mutants can alter mitochondrial respiration. Our data suggest that this change in localization is plausibly due to enhanced interaction with mitochondrial import machinery or associated chaperones, as a result of a change in protein conformation or stability. This is further supported by our analysis of the

interactome of $SHP2^{WT}$ in presence on an allosteric inhibitor, TNO155. We show that TNO155, which stabilizes SHP2 in the auto-inhibited state, shows a reduced mitochondrial signal compared to $SHP2^{WT}$. However, we note that some SHP2 mutants with decreased thermal stability do not appear to have increased mitochondrial localization, suggesting that there is nuance to the molecular mechanism of SHP2 mitochondrial import. These observations motivate further studies probing SHP2 mislocalization and mitochondrial dysregulation. More broadly, our work lays the foundation for new avenues of investigation into SHP2 signaling and pathogenicity. Ultimately, we envision that the experimental framework laid out in this study will be useful for the unbiased dissection of mutational effects in other disease-relevant proteins.

Acknowledgements

We would like to thank the members of the Shah and Jovanovic labs for their scientific insights and helpful discussions. This research was funded by NIH/NIGMS grant R35GM138014 to NHS. MJ was supported by NIH/NIGMS grant R35GM152258. LCT is supported by an NSF Graduate Research Fellowship (award # 2036197).

Author contributions

AEV conceived, designed, performed, analyzed, and interpreted the experiments; performed statistical analysis; and wrote the manuscript. LCT designed experiments and advised on interpretation and analysis of the data. ZJ, AI, and RV performed experiments. KK analyzed the data and interpreted the experiments. JTG contributed key resources. MJ designed and interpreted the experiments and edited the manuscript. NHS designed, analyzed, and interpreted the experiments, and wrote the manuscript.

Competing interests

The authors declare no competing interests.

Data and materials availability

All of the processed data, including $\log_2$ intensities from the AP-MS, TurboID-MS and corresponding total proteomes, and the enrichment scores from the high-throughput SH2 specificity screens are provided as supplementary table files. The microscopy images and deep-sequencing data from specificity screens are available as a Dryad repository (DOI: 10.5061/dryad.wstqjq2xv). Raw mass spectrometry data will be made available via ProteomeXchange. Plasmids and DNA libraries generated in this study will be made freely available upon request. There are no restrictions to the availability of data and reagents generated in this study.

Supplementary Information

Supplementary Information file contains:

Supp. Fig. 1. Affinity-purification mass spectrometry with $SHP2^{WT}$ and $SHP2^{T42A}$
Supp. Fig. 2. Quality control and validation of the SHP2-TurboID system
Supp. Fig. 3. STRING interaction networks for $SHP2^{WT}$-TurboID hits
Supp. Fig. 4. Mutation- and EGF-dependent changes in SHP2-TurboID proximity labeling
Supp. Fig. 5. STRING interaction networks for core SHP2 interactomes
Supp. Fig. 6. Mitochondrial localization of SHP2
Supp. Fig. 7. SHP2 proximity labeling distributions in subcellular compartments
Supp. Fig. 8. Mutant-specific labeling of mitochondrial import proteins and chaperones
Materials and Methods

Supplementary tables can be found as separate spreadsheet files:

Supp. Table 1. $SHP2^{WT}$ and $SHP2^{T42A}$ affinity-purification and mass spectrometry results
Supp. Table 2. TurboID fold-changes and p-values for all SHP2 variants and all conditions
Supp. Table 3. Protein abundance from total cell lysates matched with TurboID samples.
Supp. Table 4. Position-weight matrices and phosphosite scoring for SHP2 N-SH2 and C-SH2 domains

References

(1) Sun, K. Y.; Bai, X.; Chen, S.; Bao, S.; Zhang, C.; Kapoor, M.; Backman, J.; Joseph, T.; Maxwell, E.; Mitra, G.; Gorovits, A.; Mansfield, A.; Boutkov, B.; Gokhale, S.; Habegger, L.; Marcketta, A.; Locke, A. E.; Ganel, L.; Hawes, A.; Kessler, M. D.; Sharma, D.; Staples, J.; Bovijn, J.; Gelfman, S.; Di Gioia, A.; Rajagopal, V. M.; Lopez, A.; Varela, J. R.; Alegre-Díaz, J.; Berumen, J.; Tapia-Conyer, R.; Kuri-Morales, P.; Torres, J.; Emberson, J.; Collins, R.; Regeneron Genetics Center; RGC Management and Leadership Team; Abecasis, G.; Coppola, G.; Deubler, A.; Economides, A.; Ferrando, A.; Lotta, L. A.; Shuldiner, A.; Siminovitch, K.; Sequencing and Lab Operations; Beechert, C.; Brian, E. D.; Cremona, L. M.; Du, H.; Forsythe, C.; Gu, Z.; Guevara, K.; Lattari, M.; Manoochehri, K.; Challa, P.; Pradhan, M.; Reynoso, R.; Schiavo, R.; Padilla, M. S.; Wang, C.; Wolf, S. E.; Clinical Informatics; Averitt, A.; Banerjee, N.; Li, D.; Malhotra, S.; Mower, J.; Sarwar, M.; Staples, J. C.; Yu, S.; Zhang, A.; Genome Informatics and Data Engineering; Bunyea, A.; Punuru, K. P.; Sreeram, S.; Eom, G.; Sultan, B.; Lanche, R.; Mahajan, V.; Austin, E.; O'Keeffe, S.; Panea, R.; Polanco, T.; Rasool, A.; Zhang, L.; Edelstein, E.; Guan, J.; Krasheninina, O.; Zarate, S.; Mansfield, A. J.; Maxwell, E. K.; Sun, K.; Analytical Genetics and Data Science; Ferreira, M. A. R.; Burch, K.; Campos, A.; Chen, L.; Choi, S.; Damask, A.; Gaynor, S.; Geraghty, B.; Ghosh, A.; Martinez, S. R.; Gillies, C.; Gurski, L.; Herman, J.; Jorgenson, E.; Kessler, M.; Kosmicki, J.; Lin, N.; Locke, A.; Nakka, P.; Landheer, K.; Delaneau, O.; Ghoussaini, M.; Mbatchou, J.; Moscati, A.; Pandey, A.; Pandit, A.; Paulding, C.; Ross, J.; Sidore, C.; Stahl, E.; Suciu, M.; VandeHaar, P.; Vedantam, S.; Vrieze, S.; Zhang, J.; Wang, R.; Wu, K.-H.; Ye, B.; Zhang, B.; Ziyatdinov, A.; Zou, Y.; Watanabe, K.; Tang, M.; Therapeutic Area Genetics; Hobbs, B.; Silver, J.; Palmer, W.; Guerreiro, R.; Joshi, A.; Baldassari, A.; Willer, C.; Graham, S.; Mayerhofer, E.; Haas, M.; Verweij, N.; Hindy, G.; De, T.; Akbari, P.; Sun, L.; Sosina, O.; Gilly, A.; Dornbos, P.; Rodriguez-Flores, J.; Riaz, M.; Tzoneva, G.; Jallow, M. W.; Alkelai, A.; Ayer, A.; Rajagopal, V.; Kumar, V.; Otto, J.; Parikshak, N.; Guvenek, A.; Bras, J.; Alvarez, S.; Brown, J.; He, J.; Khiabanian, H.; Revez, J.; Skead, K.; Zavala, V.; Research Program Management and Strategic Initiatives; Mitnaul, L. J.; Jones, M. B.; Chen, E.; LeBlanc, M. G.; Mighty, J.; Nishtala, N.; Rana, N.; Rico-Varela, J.; Hernandez, J.; Senior Partnerships and Business Operations; Fenney, A.; Schwartz, R.; Hankins, J.; Hart, S.; Business Operations and Administrative Coordinators; Perez-Beals, A.; Solari, G.; Rivera-Picart, J.; Pagan, M.; Siceron, S.; RGC-ME Cohort Partners; Accelerated Cures; Gwynne, D.; African Descent and Glaucoma Evaluation Study (ADAGES) III; Rotter, J. I.; Weinreb, R.; Age-related macular degeneration in the Amish; Haines, J. L.; Pericak-Vance, M. A.; Stambolian, D.; Albert Einstein College of Medicine; Barzilai, N.; Suh, Y.; Zhang, Z.; Amish Connectome Project; Hong, E.; Amish Research Clinic; Mitchell, B.; The Australia and New Zealand MS Genetics Consortium; Blackburn, N. B.; Broadley, S.; Fabis-Pedrini, M. J.; Jokubaitis, V. G.; Kermode, A. G.; Kilpatrick, T. J.; Lechner-Scott, J.; Leslie, S.; McComish, B. J.; Motyer, A.; Parnell, G. P.; Scott, R. J.; Taylor, B. V.; Rubio, J. P.; Center for Non-Communicable Diseases (CNCD); Saleheen, D.; Cincinnati Children's Hospital; Kaufman, K.; Kottyan, L.; Martin, L.; Rothenberg, M. E.; Columbia University; Ali, A.; Raza, A.; Dallas Heart Study; Cohen, J.; Diabetic Retinopathy Clinical Research (DRCR) Retina Network; Glassman, A.; Duke University; Kraus, W. E.; Newgard, C. B.; Shah, S. H.; Flinders University of South Australia; Craig, J.; Hewitt, A.; Indiana Biobank; Chalasani, N.; Foroud, T.; Liangpunsakul, S.; Indiana University School of Medicine; Cox, N. J.; Dolan, E.; El-Charif, O.; Travis, L. B.; Wheeler, H.; Gamazon, E.; Kaiser Permanente; Sakoda, L.; Witte, J.; Mayo Clinic; Lazaridis, K.; Mexico City Prospective Study (MCPS); MyCode-DiscovEHR Geisinger Health System Biobank; Buchanan, A.; Carey, D. J.; Martin, C. L.; Meyer, M. N.; Retterer, K.; Rolston, D.; National Institute of Mental Health; Akula, N.; Besançon, E.; Detera-Wadleigh, S. D.; Kassem, L.; McMahon, F. J.; Schulze, T. G.; Northwestern University; Gordon, A.; Smith, M.; Varga, J.; Penn Medicine Biobank; Bradford, Y.; Damrauer, S.; DerOhannessian, S.; Drivas, T.; Dudek, S.; Dunn, J.; Haubein, N.; Judy, R.; Ko, Y.-A.; Kripke, C. M.; Livingstone, M.; Naseer, N.; Nerz, K. P.; Poindexter, A.; Risman, M.; Santos, S.; Sirugo, G.; Stephanowski, J.; Tran, T.; Vadivieso, F.; Verma, A.; Verma, S. S.; Weaver, J.; Wollack, C.; Rader, D. J.; Ritchie, M.; Primary Open-Angle African American Glaucoma Genetics (POAAG) study; O'Brien, J.; Regeneron–Mt. Sinai BioMe Biobank; Bottinger, E.; Cho, J.; UAB GWAS in African Americans with rheumatoid arthritis; Bridges, S. L.; UAB Whole exome sequencing of systemic lupus erythematosus patients;

Kimberly, R.; University of California, Los Angeles; Fejzo, M.; University of Colorado School of Medicine; Spritz, R. A.; University of Michigan Medical School; Elder, J. T.; Nair, R. P.; Stuart, P.; Tsoi, L. C.; University of Ottawa; Dent, R.; McPherson, R.; University of Pennsylvania; Keating, B.; University of Pittsburgh; Kershaw, E. E.; Papachristou, G.; Whitcomb, D. C.; University of Texas Health Science Center at Houston; Assassi, S.; Mayes, M. D.; Vanderbilt University Medical Center; Austin, E. D.; Cantor, M.; Thornton, T.; Kang, H. M.; Overton, J. D.; Shuldiner, A. R.; Cremona, M. L.; Nafde, M.; Baras, A.; Abecasis, G.; Marchini, J.; Reid, J. G.; Salerno, W.; Balasubramanian, S. A Deep Catalogue of Protein-Coding Variation in 983,578 Individuals. *Nature* **2024**, *631* (8021), 583–592. https://doi.org/10.1038/s41586-024-07556-0.

(2) Landrum, M. J.; Lee, J. M.; Riley, G. R.; Jang, W.; Rubinstein, W. S.; Church, D. M.; Maglott, D. R. ClinVar: Public Archive of Relationships among Sequence Variation and Human Phenotype. *Nucleic Acids Res* **2014**, *42* (Database issue), D980-985. https://doi.org/10.1093/nar/gkt1113.

(3) Stefl, S.; Nishi, H.; Petukh, M.; Panchenko, A. R.; Alexov, E. Molecular Mechanisms of Disease-Causing Missense Mutations. *Journal of Molecular Biology* **2013**, *425* (21), 3919–3936. https://doi.org/10.1016/j.jmb.2013.07.014.

(4) Nussinov, R.; Tsai, C.-J.; Jang, H. Autoinhibition Can Identify Rare Driver Mutations and Advise Pharmacology. *The FASEB Journal* **2020**, *34* (1), 16–29. https://doi.org/10.1096/fj.201901341R.

(5) Simanshu, D. K.; Nissley, D. V.; McCormick, F. RAS Proteins and Their Regulators in Human Disease. *Cell* **2017**, *170* (1), 17–33. https://doi.org/10.1016/j.cell.2017.06.009.

(6) Creixell, P.; Schoof, E. M.; Simpson, C. D.; Longden, J.; Miller, C. J.; Lou, H. J.; Perryman, L.; Cox, T. R.; Zivanovic, N.; Palmeri, A.; Wesolowska-Andersen, A.; Helmer-Citterich, M.; Ferkinghoff-Borg, J.; Itamochi, H.; Bodenmiller, B.; Erler, J. T.; Turk, B. E.; Linding, R. Kinome-Wide Decoding of Network-Attacking Mutations Rewiring Cancer Signaling. *Cell* **2015**, *163* (1), 202–217. https://doi.org/10.1016/j.cell.2015.08.056.

(7) van Vlimmeren, A. E.; Voleti, R.; Chartier, C. A.; Jiang, Z.; Karandur, D.; Humphries, P. A.; Lo, W.-L.; Shah, N. H. The Pathogenic T42A Mutation in SHP2 Rewires the Interaction Specificity of Its N-Terminal Regulatory Domain. *Proc Natl Acad Sci U S A* **2024**, *121* (30), e2407159121. https://doi.org/10.1073/pnas.2407159121.

(8) Lacoste, J.; Haghighi, M.; Haider, S.; Reno, C.; Lin, Z.-Y.; Segal, D.; Qian, W. W.; Xiong, X.; Teelucksingh, T.; Miglietta, E.; Shafqat-Abbasi, H.; Ryder, P. V.; Senft, R.; Cimini, B. A.; Murray, R. R.; Nyirakanani, C.; Hao, T.; McClain, G. G.; Roth, F. P.; Calderwood, M. A.; Hill, D. E.; Vidal, M.; Yi, S. S.; Sahni, N.; Peng, J.; Gingras, A.-C.; Singh, S.; Carpenter, A. E.; Taipale, M. Pervasive Mislocalization of Pathogenic Coding Variants Underlying Human Disorders. *Cell* **2024**, *187* (23), 6725-6741.e13. https://doi.org/10.1016/j.cell.2024.09.003.

(9) McConville, B. M.; Thomas, T.; Beckner, R.; Valadez, C.; Chook, Y.; Chung, S.; Liszczak, G. Enigmatic Missense Mutations Can Cause Disease via Creation of de Novo Nuclear Export Signals. bioRxiv April 24, 2024, p 2024.04.24.590854. https://doi.org/10.1101/2024.04.24.590854.

(10) Cantley, L. C.; Neel, B. G. New Insights into Tumor Suppression: PTEN Suppresses Tumor Formation by Restraining the Phosphoinositide 3-Kinase/AKT Pathway. *Proc. Natl. Acad. Sci. U.S.A.* **1999**, *96* (8), 4240–4245. https://doi.org/10.1073/pnas.96.8.4240.

(11) Keniry, M.; Parsons, R. The Role of PTEN Signaling Perturbations in Cancer and in Targeted Therapy. *Oncogene* **2008**, *27* (41), 5477–5485. https://doi.org/10.1038/onc.2008.248.

(12) Yu, L.; Wang, C.; Pan, F.; Liu, Y.; Ren, X.; Zeng, H.; Shi, Y. HePTP Promotes Migration and Invasion in Triple-Negative Breast Cancer Cells via Activation of Wnt/β-Catenin Signaling. *Biomedicine & Pharmacotherapy* **2019**, *118*, 109361. https://doi.org/10.1016/j.biopha.2019.109361.

(13) Zhang, Q.; Wang, H. Y.; Marzec, M.; Raghunath, P. N.; Nagasawa, T.; Wasik, M. A. STAT3- and DNA Methyltransferase 1-Mediated Epigenetic Silencing of SHP-1 Tyrosine Phosphatase Tumor

Suppressor Gene in Malignant T Lymphocytes. *Proc. Natl. Acad. Sci. U.S.A.* **2005**, *102* (19), 6948–6953. https://doi.org/10.1073/pnas.0501959102.

(14) Julien, S. G.; Dubé, N.; Hardy, S.; Tremblay, M. L. Inside the Human Cancer Tyrosine Phosphatome. *Nat Rev Cancer* **2011**, *11* (1), 35–49. https://doi.org/10.1038/nrc2980.

(15) Tonks, N. K. Protein Tyrosine Phosphatases – from Housekeeping Enzymes to Master Regulators of Signal Transduction. *The FEBS Journal* **2013**, *280* (2), 346–378. https://doi.org/10.1111/febs.12077.

(16) Salmond, R. J.; Alexander, D. R. SHP2 Forecast for the Immune System: Fog Gradually Clearing. *Trends in Immunology* **2006**, *27* (3), 154–160. https://doi.org/10.1016/j.it.2006.01.007.

(17) Lauriol, J.; Jaffré, F.; Kontaridis, M. I. The Role of the Protein Tyrosine Phosphatase SHP2 in Cardiac Development and Disease. *Seminars in Cell & Developmental Biology* **2015**, *37*, 73–81. https://doi.org/10.1016/j.semcdb.2014.09.013.

(18) Asmamaw, M. D.; Shi, X.-J.; Zhang, L.-R.; Liu, H.-M. A Comprehensive Review of SHP2 and Its Role in Cancer. *Cell Oncol.* **2022**, *45* (5), 729–753. https://doi.org/10.1007/s13402-022-00698-1.

(19) Agazie, Y. M.; Hayman, M. J. Molecular Mechanism for a Role of SHP2 in Epidermal Growth Factor Receptor Signaling. *Molecular and Cellular Biology* **2003**, *23* (21), 7875–7886. https://doi.org/10.1128/MCB.23.21.7875-7886.2003.

(20) Hof, P.; Pluskey, S.; Dhe-Paganon, S.; Eck, M. J.; Shoelson, S. E. Crystal Structure of the Tyrosine Phosphatase SHP-2. *Cell* **1998**, *92* (4), 441–450. https://doi.org/10.1016/S0092-8674(00)80938-1.

(21) Marasco, M.; Berteotti, A.; Weyershaeuser, J.; Thorausch, N.; Sikorska, J.; Krausze, J.; Brandt, H. J.; Kirkpatrick, J.; Rios, P.; Schamel, W. W.; Köhn, M.; Carlomagno, T. Molecular Mechanism of SHP2 Activation by PD-1 Stimulation. *Science Advances* **2020**, *6* (5), eaay4458. https://doi.org/10.1126/sciadv.aay4458.

(22) Tartaglia, M.; Mehler, E. L.; Goldberg, R.; Zampino, G.; Brunner, H. G.; Kremer, H.; Van Der Burgt, I.; Crosby, A. H.; Ion, A.; Jeffery, S.; Kalidas, K.; Patton, M. A.; Kucherlapati, R. S.; Gelb, B. D. Mutations in PTPN11, Encoding the Protein Tyrosine Phosphatase SHP-2, Cause Noonan Syndrome. *Nat Genet* **2001**, *29* (4), 465–468. https://doi.org/10.1038/ng772.

(23) Keilhack, H.; David, F. S.; McGregor, M.; Cantley, L. C.; Neel, B. G. Diverse Biochemical Properties of Shp2 Mutants. *Journal of Biological Chemistry* **2005**, *280* (35), 30984–30993. https://doi.org/10.1074/jbc.M504699200.

(24) Grossmann, K. S.; Rosário, M.; Birchmeier, C.; Birchmeier, W. The Tyrosine Phosphatase Shp2 in Development and Cancer. In *Advances in Cancer Research*; Elsevier, 2010; Vol. 106, pp 53–89. https://doi.org/10.1016/S0065-230X(10)06002-1.

(25) Edouard, T.; Combier, J.-P.; Nédélec, A.; Bel-Vialar, S.; Métrich, M.; Conte-Auriol, F.; Lyonnet, S.; Parfait, B.; Tauber, M.; Salles, J.-P.; Lezoualc'h, F.; Yart, A.; Raynal, P. Functional Effects of *PTPN11* (SHP2) Mutations Causing LEOPARD Syndrome on Epidermal Growth Factor-Induced Phosphoinositide 3-Kinase/AKT/Glycogen Synthase Kinase 3β Signaling. *Molecular and Cellular Biology* **2010**, *30* (10), 2498–2507. https://doi.org/10.1128/MCB.00646-09.

(26) Nabinger, S. C.; Li, X. J.; Ramdas, B.; He, Y.; Zhang, X.; Zeng, L.; Richine, B.; Bowling, J. D.; Fukuda, S.; Goenka, S.; Liu, Z.; Feng, G.-S.; Yu, M.; Sandusky, G. E.; Boswell, H. S.; Zhang, Z.-Y.; Kapur, R.; Chan, R. J. The Protein Tyrosine Phosphatase, Shp2, Positively Contributes to FLT3-ITD-Induced Hematopoietic Progenitor Hyperproliferation and Malignant Disease in Vivo. *Leukemia* **2013**, *27* (2), 398–408. https://doi.org/10.1038/leu.2012.308.

(27) Furcht, C. M.; Muñoz Rojas, A. R.; Nihalani, D.; Lazzara, M. J. Diminished Functional Role and Altered Localization of SHP2 in Non-Small Cell Lung Cancer Cells with EGFR-Activating Mutations. *Oncogene* **2013**, *32* (18), 2346–2355. https://doi.org/10.1038/onc.2012.240.

(28) Roberts, A. E.; Allanson, J. E.; Tartaglia, M.; Gelb, B. D. Noonan Syndrome. *The Lancet* **2013**, *381* (9863), 333–342. https://doi.org/10.1016/S0140-6736(12)61023-X.

(29) Gelb, B. D.; Tartaglia, M. Noonan Syndrome with Multiple Lentigines. In *GeneReviews®*; Adam, M. P., Feldman, J., Mirzaa, G. M., Pagon, R. A., Wallace, S. E., Amemiya, A., Eds.; University of Washington, Seattle: Seattle (WA), 1993.

(30) Bentires-Alj, M.; Paez, J. G.; David, F. S.; Keilhack, H.; Halmos, B.; Naoki, K.; Maris, J. M.; Richardson, A.; Bardelli, A.; Sugarbaker, D. J.; Richards, W. G.; Du, J.; Girard, L.; Minna, J. D.; Loh, M. L.; Fisher, D. E.; Velculescu, V. E.; Vogelstein, B.; Meyerson, M.; Sellers, W. R.; Neel, B. G. Activating Mutations of the Noonan Syndrome-Associated ***SHP2/PTPN11*** Gene in Human Solid Tumors and Adult Acute Myelogenous Leukemia. *Cancer Research* **2004**, *64* (24), 8816–8820. https://doi.org/10.1158/0008-5472.CAN-04-1923.

(31) Scheiter, A.; Lu, L.-C.; Gao, L. H.; Feng, G.-S. Complex Roles of PTPN11/SHP2 in Carcinogenesis and Prospect of Targeting SHP2 in Cancer Therapy. *Annual Review of Cancer Biology* **2024**, *8* (1), 15–33. https://doi.org/10.1146/annurev-cancerbio-062722-013740.

(32) Walter, A. O.; Peng, Z.-Y.; Cartwright, C. A. The Shp-2 Tyrosine Phosphatase Activates the Src Tyrosine Kinase by a Non-Enzymatic Mechanism. *Oncogene* **1999**, *18* (11), 1911–1920. https://doi.org/10.1038/sj.onc.1202513.

(33) Paardekooper Overman, J.; Yi, J.-S.; Bonetti, M.; Soulsby, M.; Preisinger, C.; Stokes, M. P.; Hui, L.; Silva, J. C.; Overvoorde, J.; Giansanti, P.; Heck, A. J. R.; Kontaridis, M. I.; den Hertog, J.; Bennett, A. M. PZR Coordinates Shp2 Noonan and LEOPARD Syndrome Signaling in Zebrafish and Mice. *Molecular and Cellular Biology* **2014**, *34* (15), 2874–2889. https://doi.org/10.1128/MCB.00135-14.

(34) Yi, J.-S.; Perla, S.; Enyenihi, L.; Bennett, A. M. Tyrosyl Phosphorylation of PZR Promotes Hypertrophic Cardiomyopathy in PTPN11-Associated Noonan Syndrome with Multiple Lentigines. *JCI Insight* **2020**, *5* (15), e137753. https://doi.org/10.1172/jci.insight.137753.

(35) Lin, C.-C.; Wieteska, L.; Suen, K. M.; Kalverda, A. P.; Ahmed, Z.; Ladbury, J. E. Grb2 Binding Induces Phosphorylation-Independent Activation of Shp2. *Commun Biol* **2021**, *4* (1), 437. https://doi.org/10.1038/s42003-021-01969-7.

(36) Jiang, Z.; Vlimmeren, A. E. van; Karandur, D.; Semmelman, A.; Shah, N. H. Deep Mutational Scanning of a Multi-Domain Signaling Protein Reveals Mechanisms of Regulation and Pathogenicity. bioRxiv November 19, 2024, p 2024.05.13.593907. https://doi.org/10.1101/2024.05.13.593907.

(37) Yu, Z.-H.; Zhang, R.-Y.; Walls, C. D.; Chen, L.; Zhang, S.; Wu, L.; Liu, S.; Zhang, Z.-Y. Molecular Basis of Gain-of-Function LEOPARD Syndrome-Associated SHP2 Mutations. *Biochemistry* **2014**, *53* (25), 4136–4151. https://doi.org/10.1021/bi5002695.

(38) Martinelli, S.; Torreri, P.; Tinti, M.; Stella, L.; Bocchinfuso, G.; Flex, E.; Grottesi, A.; Ceccarini, M.; Palleschi, A.; Cesareni, G.; Castagnoli, L.; Petrucci, T. C.; Gelb, B. D.; Tartaglia, M. Diverse Driving Forces Underlie the Invariant Occurrence of the T42A, E139D, I282V and T468M SHP2 Amino Acid Substitutions Causing Noonan and LEOPARD Syndromes. *Hum Mol Genet* **2008**, *17* (13), 2018–2029. https://doi.org/10.1093/hmg/ddn099.

(39) Zhu, G.; Xie, J.; Kong, W.; Xie, J.; Li, Y.; Du, L.; Zheng, Q.; Sun, L.; Guan, M.; Li, H.; Zhu, T.; He, H.; Liu, Z.; Xia, X.; Kan, C.; Tao, Y.; Shen, H. C.; Li, D.; Wang, S.; Yu, Y.; Yu, Z.-H.; Zhang, Z.-Y.; Liu, C.; Zhu, J. Phase Separation of Disease-Associated SHP2 Mutants Underlies MAPK Hyperactivation. *Cell* **2020**, *183* (2), 490-502.e18. https://doi.org/10.1016/j.cell.2020.09.002.

(40) Zhang, R.-Y.; Yu, Z.-H.; Chen, L.; Walls, C. D.; Zhang, S.; Wu, L.; Zhang, Z.-Y. Mechanistic Insights Explain the Transforming Potential of the T507K Substitution in the Protein-Tyrosine Phosphatase SHP2. *Journal of Biological Chemistry* **2020**, *295* (18), 6187–6201. https://doi.org/10.1074/jbc.RA119.010274.

(41) St-Denis, N.; Gupta, G. D.; Lin, Z. Y.; Gonzalez-Badillo, B.; Veri, A. O.; Knight, J. D. R.; Rajendran, D.; Couzens, A. L.; Currie, K. W.; Tkach, J. M.; Cheung, S. W. T.; Pelletier, L.; Gingras, A.-C. Phenotypic and Interaction Profiling of the Human Phosphatases Identifies Diverse Mitotic Regulators. *Cell Reports* **2016**, *17* (9), 2488–2501. https://doi.org/10.1016/j.celrep.2016.10.078.

(42) Westermarck, J.; Ivaska, J.; Corthals, G. L. Identification of Protein Interactions Involved in Cellular Signaling. *Molecular & Cellular Proteomics* **2013**, *12* (7), 1752–1763. https://doi.org/10.1074/mcp.R113.027771.

(43) Stanford, S. M.; Ahmed, V.; Barrios, A. M.; Bottini, N. Cellular Biochemistry Methods for Investigating Protein Tyrosine Phosphatases. *Antioxidants & Redox Signaling* **2014**, *20* (14), 2160–2178. https://doi.org/10.1089/ars.2013.5731.

(44) Oh, D.; Ogiue-Ikeda, M.; Jadwin, J. A.; Machida, K.; Mayer, B. J.; Yu, J. Fast Rebinding Increases Dwell Time of Src Homology 2 (SH2)-Containing Proteins near the Plasma Membrane. *Proceedings of the National Academy of Sciences* **2012**, *109* (35), 14024–14029. https://doi.org/10.1073/pnas.1203397109.

(45) Branon, T. C.; Bosch, J. A.; Sanchez, A. D.; Udeshi, N. D.; Svinkina, T.; Carr, S. A.; Feldman, J. L.; Perrimon, N.; Ting, A. Y. Efficient Proximity Labeling in Living Cells and Organisms with TurboID. *Nat Biotechnol* **2018**, *36* (9), 880–887. https://doi.org/10.1038/nbt.4201.

(46) St-Denis, N.; Gupta, G. D.; Lin, Z. Y.; Gonzalez-Badillo, B.; Veri, A. O.; Knight, J. D. R.; Rajendran, D.; Couzens, A. L.; Currie, K. W.; Tkach, J. M.; Cheung, S. W. T.; Pelletier, L.; Gingras, A.-C. Phenotypic and Interaction Profiling of the Human Phosphatases Identifies Diverse Mitotic Regulators. *Cell Reports* **2016**, *17* (9), 2488–2501. https://doi.org/10.1016/j.celrep.2016.10.078.

(47) Fearnley, G. W.; Young, K. A.; Edgar, J. R.; Antrobus, R.; Hay, I. M.; Liang, W.-C.; Martinez-Martin, N.; Lin, W.; Deane, J. E.; Sharpe, H. J. The Homophilic Receptor PTPRK Selectively Dephosphorylates Multiple Junctional Regulators to Promote Cell-Cell Adhesion. *Elife* **2019**, *8*, e44597. https://doi.org/10.7554/eLife.44597.

(48) Gong, Y.; Abudureyimu, S.; Kadomatsu, K.; Sakamoto, K. Identification of PTPRσ-Interacting Proteins by Proximity-Labelling Assay. *The Journal of Biochemistry* **2021**, *169* (2), 187–194. https://doi.org/10.1093/jb/mvaa141.

(49) Zhu, P.; Wu, X.; Zhang, R.-Y.; Hsu, C.-C.; Zhang, Z.-Y.; Tao, W. A. An Integrated Proteomic Strategy to Identify SHP2 Substrates. *J. Proteome Res.* **2022**, *21* (10), 2515–2525. https://doi.org/10.1021/acs.jproteome.2c00481.

(50) Cho, K. F.; Branon, T. C.; Udeshi, N. D.; Myers, S. A.; Carr, S. A.; Ting, A. Y. Proximity Labeling in Mammalian Cells with TurboID and Split-TurboID. *Nat Protoc* **2020**, *15* (12), 3971–3999. https://doi.org/10.1038/s41596-020-0399-0.

(51) Takahashi, A.; Tsutsumi, R.; Kikuchi, I.; Obuse, C.; Saito, Y.; Seidi, A.; Karisch, R.; Fernandez, M.; Cho, T.; Ohnishi, N.; Rozenblatt-Rosen, O.; Meyerson, M.; Neel, B. G.; Hatakeyama, M. SHP2 Tyrosine Phosphatase Converts Parafibromin/Cdc73 from a Tumor Suppressor to an Oncogenic Driver. *Molecular Cell* **2011**, *43* (1), 45–56. https://doi.org/10.1016/j.molcel.2011.05.014.

(52) Shi, Z.-Q.; Yu, D.-H.; Park, M.; Marshall, M.; Feng, G.-S. Molecular Mechanism for the Shp-2 Tyrosine Phosphatase Function in Promoting Growth Factor Stimulation of Erk Activity. *Molecular and Cellular Biology* **2000**, *20* (5), 1526–1536. https://doi.org/10.1128/MCB.20.5.1526-1536.2000.

(53) Schaeper, U.; Gehring, N. H.; Fuchs, K. P.; Sachs, M.; Kempkes, B.; Birchmeier, W. Coupling of Gab1 to C-Met, Grb2, and Shp2 Mediates Biological Responses. *The Journal of Cell Biology* **2000**, *149* (7), 1419–1432. https://doi.org/10.1083/jcb.149.7.1419.

(54) Cunnick, J. M.; Dorsey, J. F.; Munoz-Antonia, T.; Mei, L.; Wu, J. Requirement of SHP2 Binding to Grb2-Associated Binder-1 for Mitogen-Activated Protein Kinase Activation in Response to

Lysophosphatidic Acid and Epidermal Growth Factor. *Journal of Biological Chemistry* **2000**, *275* (18), 13842–13848. https://doi.org/10.1074/jbc.275.18.13842.

(55) Havugimana, P. C.; Hart, G. T.; Nepusz, T.; Yang, H.; Turinsky, A. L.; Li, Z.; Wang, P. I.; Boutz, D. R.; Fong, V.; Phanse, S.; Babu, M.; Craig, S. A.; Hu, P.; Wan, C.; Vlasblom, J.; Dar, V.-N.; Bezginov, A.; Clark, G. W.; Wu, G. C.; Wodak, S. J.; Tillier, E. R. M.; Paccanaro, A.; Marcotte, E. M.; Emili, A. A Census of Human Soluble Protein Complexes. *Cell* **2012**, *150* (5), 1068–1081. https://doi.org/10.1016/j.cell.2012.08.011.

(56) Huttlin, E. L.; Bruckner, R. J.; Navarrete-Perea, J.; Cannon, J. R.; Baltier, K.; Gebreab, F.; Gygi, M. P.; Thornock, A.; Zarraga, G.; Tam, S.; Szpyt, J.; Gassaway, B. M.; Panov, A.; Parzen, H.; Fu, S.; Golbazi, A.; Maenpaa, E.; Stricker, K.; Guha Thakurta, S.; Zhang, T.; Rad, R.; Pan, J.; Nusinow, D. P.; Paulo, J. A.; Schweppe, D. K.; Vaites, L. P.; Harper, J. W.; Gygi, S. P. Dual Proteome-Scale Networks Reveal Cell-Specific Remodeling of the Human Interactome. *Cell* **2021**, *184* (11), 3022-3040.e28. https://doi.org/10.1016/j.cell.2021.04.011.

(57) Brehme, M.; Hantschel, O.; Colinge, J.; Kaupe, I.; Planyavsky, M.; Köcher, T.; Mechtler, K.; Bennett, K. L.; Superti-Furga, G. Charting the Molecular Network of the Drug Target Bcr-Abl. *Proceedings of the National Academy of Sciences* **2009**, *106* (18), 7414–7419. https://doi.org/10.1073/pnas.0900653106.

(58) de Kreuk, B.-J.; Anthony, E. C.; Geerts, D.; Hordijk, P. L. The F-BAR Protein PACSIN2 Regulates Epidermal Growth Factor Receptor Internalization. *J Biol Chem* **2012**, *287* (52), 43438–43453. https://doi.org/10.1074/jbc.M112.391078.

(59) Kourtidis, A.; Necela, B.; Lin, W.-H.; Lu, R.; Feathers, R. W.; Asmann, Y. W.; Thompson, E. A.; Anastasiadis, P. Z. Cadherin Complexes Recruit mRNAs and RISC to Regulate Epithelial Cell Signaling. *J Cell Biol* **2017**, *216* (10), 3073–3085. https://doi.org/10.1083/jcb.201612125.

(60) Mei, Y.; Hahn, A. A.; Hu, S.; Yang, X. The USP19 Deubiquitinase Regulates the Stability of C-IAP1 and c-IAP2. *J Biol Chem* **2011**, *286* (41), 35380–35387. https://doi.org/10.1074/jbc.M111.282020.

(61) Tan, B. M.; Zammit, N. W.; Yam, A. O.; Slattery, R.; Walters, S. N.; Malle, E.; Grey, S. T. Baculoviral Inhibitors of Apoptosis Repeat Containing (BIRC) Proteins Fine-Tune TNF-Induced Nuclear Factor κB and c-Jun N-Terminal Kinase Signalling in Mouse Pancreatic Beta Cells. *Diabetologia* **2013**, *56* (3), 520–532. https://doi.org/10.1007/s00125-012-2784-x.

(62) Hornbeck, P. V.; Kornhauser, J. M.; Latham, V.; Murray, B.; Nandhikonda, V.; Nord, A.; Skrzypek, E.; Wheeler, T.; Zhang, B.; Gnad, F. 15 Years of PhosphoSitePlus®: Integrating Post-Translationally Modified Sites, Disease Variants and Isoforms. *Nucleic Acids Research* **2019**, *47* (D1), D433–D441. https://doi.org/10.1093/nar/gky1159.

(63) Li, A.; Voleti, R.; Lee, M.; Gagoski, D.; Shah, N. H. High-Throughput Profiling of Sequence Recognition by Tyrosine Kinases and SH2 Domains Using Bacterial Peptide Display. *eLife* **2023**, *12*, e82345. https://doi.org/10.7554/eLife.82345.

(64) An, S. J.; Anneken, A.; Xi, Z.; Choi, C.; Schlessinger, J.; Toomre, D. Regulation of EGF-Stimulated Activation of the PI-3K/AKT Pathway by Exocyst-Mediated Exocytosis. *Proc Natl Acad Sci U S A* **2022**, *119* (48), e2208947119. https://doi.org/10.1073/pnas.2208947119.

(65) Li, H.; Zhang, M.; Wei, Y.; Haider, F.; Lin, Y.; Guan, W.; Liu, Y.; Zhang, S.; Yuan, R.; Yang, X.; Yang, S.; Wang, H. SH3BGRL Confers Innate Drug Resistance in Breast Cancer by Stabilizing HER2 Activation on Cell Membrane. *J Exp Clin Cancer Res* **2020**, *39* (1), 81. https://doi.org/10.1186/s13046-020-01577-z.

(66) Toto, A.; Malagrinò, F.; Visconti, L.; Troilo, F.; Gianni, S. Unveiling the Molecular Basis of the Noonan Syndrome-Causing Mutation T42A of SHP2. *IJMS* **2020**, *21* (2), 461. https://doi.org/10.3390/ijms21020461.

(67) Pádua, R. A. P.; Sun, Y.; Marko, I.; Pitsawong, W.; Stiller, J. B.; Otten, R.; Kern, D. Mechanism of Activating Mutations and Allosteric Drug Inhibition of the Phosphatase SHP2. *Nature Communications* **2018**, *9* (1), 4507. https://doi.org/10.1038/s41467-018-06814-w.

(68) LaRochelle, J. R.; Fodor, M.; Vemulapalli, V.; Mohseni, M.; Wang, P.; Stams, T.; LaMarche, M. J.; Chopra, R.; Acker, M. G.; Blacklow, S. C. Structural Reorganization of SHP2 by Oncogenic Mutations and Implications for Oncoprotein Resistance to Allosteric Inhibition. *Nat Commun* **2018**, *9* (1), 4508. https://doi.org/10.1038/s41467-018-06823-9.

(69) Yu, Z.-H.; Xu, J.; Walls, C. D.; Chen, L.; Zhang, S.; Zhang, R.; Wu, L.; Wang, L.; Liu, S.; Zhang, Z.-Y. Structural and Mechanistic Insights into LEOPARD Syndrome-Associated SHP2 Mutations. *The Journal of Biological Chemistry* **2013**, *288* (15), 10472–10482. https://doi.org/10.1074/jbc.M113.450023.

(70) Vemulapalli, V.; Chylek, L. A.; Erickson, A.; Pfeiffer, A.; Gabriel, K.-H.; LaRochelle, J.; Subramanian, K.; Cao, R.; Stegmaier, K.; Mohseni, M.; LaMarche, M. J.; Acker, M. G.; Sorger, P. K.; Gygi, S. P.; Blacklow, S. C. Time-Resolved Phosphoproteomics Reveals Scaffolding and Catalysis-Responsive Patterns of SHP2-Dependent Signaling. *eLife* **2021**, *10*, e64251. https://doi.org/10.7554/eLife.64251.

(71) Salvi, M.; Stringaro, A.; Brunati, A. M.; Agostinelli, E.; Arancia, G.; Clari, G.; Toninello, A. Tyrosine Phosphatase Activity in Mitochondria: Presence of Shp-2 Phosphatase in Mitochondria. *Cell Mol Life Sci* **2004**, *61* (18), 2393–2404. https://doi.org/10.1007/s00018-004-4211-z.

(72) Arachiche, A.; Augereau, O.; Decossas, M.; Pertuiset, C.; Gontier, E.; Letellier, T.; Dachary-Prigent, J. Localization of PTP-1B, SHP-2, and Src Exclusively in Rat Brain Mitochondria and Functional Consequences. *J Biol Chem* **2008**, *283* (36), 24406–24411. https://doi.org/10.1074/jbc.M709217200.

(73) Zang, Q. S.; Martinez, B.; Yao, X.; Maass, D. L.; Ma, L.; Wolf, S. E.; Minei, J. P. Sepsis-Induced Cardiac Mitochondrial Dysfunction Involves Altered Mitochondrial-Localization of Tyrosine Kinase Src and Tyrosine Phosphatase SHP2. *PLoS One* **2012**, *7* (8), e43424. https://doi.org/10.1371/journal.pone.0043424.

(74) Xu, D.; Zheng, H.; Yu, W.-M.; Qu, C.-K. Activating Mutations in Protein Tyrosine Phosphatase Ptpn11 (Shp2) Enhance Reactive Oxygen Species Production That Contributes to Myeloproliferative Disorder. *PLOS ONE* **2013**, *8* (5), e63152. https://doi.org/10.1371/journal.pone.0063152.

(75) Guo, W.; Liu, W.; Chen, Z.; Gu, Y.; Peng, S.; Shen, L.; Shen, Y.; Wang, X.; Feng, G.-S.; Sun, Y.; Xu, Q. Tyrosine Phosphatase SHP2 Negatively Regulates NLRP3 Inflammasome Activation via ANT1-Dependent Mitochondrial Homeostasis. *Nature Communications* **2017**, *8* (1), 2168. https://doi.org/10.1038/s41467-017-02351-0.

(76) Morgenstern, M.; Peikert, C. D.; Lübbert, P.; Suppanz, I.; Klemm, C.; Alka, O.; Steiert, C.; Naumenko, N.; Schendzielorz, A.; Melchionda, L.; Mühlhäuser, W. W. D.; Knapp, B.; Busch, J. D.; Stiller, S. B.; Dannenmaier, S.; Lindau, C.; Licheva, M.; Eickhorst, C.; Galbusera, R.; Zerbes, R. M.; Ryan, M. T.; Kraft, C.; Kozjak-Pavlovic, V.; Drepper, F.; Dennerlein, S.; Oeljeklaus, S.; Pfanner, N.; Wiedemann, N.; Warscheid, B. Quantitative High-Confidence Human Mitochondrial Proteome and Its Dynamics in Cellular Context. *Cell Metab* **2021**, *33* (12), 2464-2483.e18. https://doi.org/10.1016/j.cmet.2021.11.001.

(77) Kan, C.; Tan, Z.; Liu, L.; Liu, B.; Zhan, L.; Zhu, J.; Li, X.; Lin, K.; Liu, J.; Liu, Y.; Yang, F.; Wong, M.; Wang, S.; Zheng, H. Phase Separation of SHP2E76K Promotes Malignant Transformation of Mesenchymal Stem Cells by Activating Mitochondrial Complexes. *JCI Insight* **2024**, *9* (8), e170340. https://doi.org/10.1172/jci.insight.170340.

(78) Petrelli, F.; Moretti, P.; Paparelli, M. Intracellular Distribution of Biotin-14COOH in Rat Liver. *Mol Biol Rep* **1978**, *4* (4), 247–252. https://doi.org/10.1007/BF00777563.

(79) Baldet, P.; Alban, C.; Axiotis, S.; Douce, R. Characterization of Biotin and 3-Methylcrotonyl-Coenzyme A Carboxylase in Higher Plant Mitochondria. *Plant Physiology* **1992**, *99* (2), 450–455. https://doi.org/10.1104/pp.99.2.450.

(80) Said, H. M.; McAlister-Henn, L.; Mohammadkhani, R.; Horne, D. W. Uptake of Biotin by Isolated Rat Liver Mitochondria. *American Journal of Physiology-Gastrointestinal and Liver Physiology* **1992**, *263* (1), G81–G86. https://doi.org/10.1152/ajpgi.1992.263.1.G81.

(81) Lee, I.; Pecinova, A.; Pecina, P.; Neel, B. G.; Araki, T.; Kucherlapati, R.; Roberts, A. E.; Huttemann, M. A Suggested Role for Mitochondria in Noonan Syndrome. *Biochim Biophys Acta* **2010**, *1802* (2), 275–283. https://doi.org/10.1016/j.bbadis.2009.10.005.

(82) Karampitsakos, T.; Galaris, A.; Barbayianni, I.; DeIuliis, G.; Ahangari, F.; Sampsonas, F.; Sotiropoulou, V.; Aidinis, V.; Bennett, A.; Herazo-Maya, J.; Xylourgidis, N.; Bakakos, P.; Bouros, D.; Kaminski, N.; Tzouvelekis, A. SH2 Domain-Containing Phosphatase-SHP2 Attenuates Fibrotic Responses through Negative Regulation of Mitochondrial Metabolism in Lung Fibroblasts. *Diagnostics* **2023**, *13* (6), 1166. https://doi.org/10.3390/diagnostics13061166.

(83) Zheng, H.; Li, S.; Hsu, P.; Qu, C.-K. Induction of a Tumor-Associated Activating Mutation in Protein Tyrosine Phosphatase Ptpn11 (Shp2) Enhances Mitochondrial Metabolism, Leading to Oxidative Stress and Senescence. *J Biol Chem* **2013**, *288* (36), 25727–25738. https://doi.org/10.1074/jbc.M113.462291.

(84) Abe, Y.; Shodai, T.; Muto, T.; Mihara, K.; Torii, H.; Nishikawa, S.; Endo, T.; Kohda, D. Structural Basis of Presequence Recognition by the Mitochondrial Protein Import Receptor Tom20. *Cell* **2000**, *100* (5), 551–560. https://doi.org/10.1016/S0092-8674(00)80691-1.

(85) Akram, S.; Zittlau, K. I.; Maček, B.; Jansen, R.-P. Proximity Labeling Reveals Differential Interaction Partners of the Human Mitochondrial Import Receptor Proteins TOMM20 and TOMM70. October 25, 2024. https://doi.org/10.1101/2024.10.25.620316.

(86) Pfanner, N.; Warscheid, B.; Wiedemann, N. Mitochondrial Proteins: From Biogenesis to Functional Networks. *Nat Rev Mol Cell Biol* **2019**, *20* (5), 267–284. https://doi.org/10.1038/s41580-018-0092-0.

(87) Yoo, J. C.; Hayman, M. J. HSP70 Binds to SHP2 and Has Effects on the SHP2-Related EGFR/GAB1 Signaling Pathway. *Biochemical and Biophysical Research Communications* **2006**, *351* (4), 979–985. https://doi.org/10.1016/j.bbrc.2006.10.152.

(88) Qiu, X.-B.; Shao, Y.-M.; Miao, S.; Wang, L. The Diversity of the DnaJ/Hsp40 Family, the Crucial Partners for Hsp70 Chaperones. *Cell Mol Life Sci* **2006**, *63* (22), 2560–2570. https://doi.org/10.1007/s00018-006-6192-6.

(89) Waingankar, T. P.; D'Silva, P. Multiple Variants of the Human Presequence Translocase Motor Subunit Magmas Govern the Mitochondrial Import. *J Biol Chem* **2021**, *297* (6), 101349. https://doi.org/10.1016/j.jbc.2021.101349.

(90) Wang, S.-F.; Huang, K.-H.; Tseng, W.-C.; Lo, J.-F.; Li, A. F.-Y.; Fang, W.-L.; Chen, C.-F.; Yeh, T.-S.; Chang, Y.-L.; Chou, Y.-C.; Hung, H.-H.; Lee, H.-C. DNAJA3/Tid1 Is Required for Mitochondrial DNA Maintenance and Regulates Migration and Invasion of Human Gastric Cancer Cells. *Cancers (Basel)* **2020**, *12* (11), 3463. https://doi.org/10.3390/cancers12113463.

(91) Violitzi, F.; Perivolidi, V.-I.; Thireou, T.; Grivas, I.; Haralambous, S.; Samiotaki, M.; Panayotou, G.; Douni, E. Mapping Interactome Networks of DNAJC11, a Novel Mitochondrial Protein Causing Neuromuscular Pathology in Mice. *J. Proteome Res.* **2019**, *18* (11), 3896–3912. https://doi.org/10.1021/acs.jproteome.9b00338.

(92) Hayashi, M.; Imanaka-Yoshida, K.; Yoshida, T.; Wood, M.; Fearns, C.; Tatake, R. J.; Lee, J.-D. A Crucial Role of Mitochondrial Hsp40 in Preventing Dilated Cardiomyopathy. *Nat Med* **2006**, *12* (1), 128–132. https://doi.org/10.1038/nm1327.

(93) Ojala, T.; Polinati, P.; Manninen, T.; Hiippala, A.; Rajantie, J.; Karikoski, R.; Suomalainen, A.; Tyni, T. New Mutation of Mitochondrial DNAJC19 Causing Dilated and Noncompaction Cardiomyopathy, Anemia, Ataxia, and Male Genital Anomalies. *Pediatr Res* **2012**, *72* (4), 432–437. https://doi.org/10.1038/pr.2012.92.

(94) Serbina, A.; Bishop, A. C. Quantitation of Autoinhibitory Defects in Pathogenic SHP2 Mutants by Differential Scanning Fluorimetry. *Analytical Biochemistry* **2023**, *680*, 115300. https://doi.org/10.1016/j.ab.2023.115300.

(95) Kim, S. H.; Bulos, M. L.; Adams, J. A.; Yun, B. K.; Bishop, A. C. Single Ion Pair Is Essential for Stabilizing SHP2's Open Conformation. *Biochemistry* **2024**, *63* (3), 273–281. https://doi.org/10.1021/acs.biochem.3c00609.

(96) Yuan, X.; Bu, H.; Zhou, J.; Yang, C.-Y.; Zhang, H. Recent Advances of SHP2 Inhibitors in Cancer Therapy: Current Development and Clinical Application. *J. Med. Chem.* **2020**, *63* (20), 11368–11396. https://doi.org/10.1021/acs.jmedchem.0c00249.

(97) Guo, Z.; Duan, Y.; Sun, K.; Zheng, T.; Liu, J.; Xu, S.; Xu, J. Advances in SHP2 Tunnel Allosteric Inhibitors and Bifunctional Molecules. *European Journal of Medicinal Chemistry* **2024**, *275*, 116579. https://doi.org/10.1016/j.ejmech.2024.116579.

(98) LaMarche, M. J.; Acker, M.; Argintaru, A.; Bauer, D.; Boisclair, J.; Chan, H.; Chen, C. H.-T.; Chen, Y.-N.; Chen, Z.; Deng, Z.; Dore, M.; Dunstan, D.; Fan, J.; Fekkes, P.; Firestone, B.; Fodor, M.; Garcia-Fortanet, J.; Fortin, P. D.; Fridrich, C.; Giraldes, J.; Glick, M.; Grunenfelder, D.; Hao, H.-X.; Hentemann, M.; Ho, S.; Jouk, A.; Kang, Z. B.; Karki, R.; Kato, M.; Keen, N.; Koenig, R.; LaBonte, L. R.; Larrow, J.; Liu, G.; Liu, S.; Majumdar, D.; Mathieu, S.; Meyer, M. J.; Mohseni, M.; Ntaganda, R.; Palermo, M.; Perez, L.; Pu, M.; Ramsey, T.; Reilly, J.; Sarver, P.; Sellers, W. R.; Sendzik, M.; Shultz, M. D.; Slisz, J.; Slocum, K.; Smith, T.; Spence, S.; Stams, T.; Straub, C.; Tamez, V.; Toure, B.-B.; Towler, C.; Wang, P.; Wang, H.; Williams, S. L.; Yang, F.; Yu, B.; Zhang, J.-H.; Zhu, S. Identification of TNO155, an Allosteric SHP2 Inhibitor for the Treatment of Cancer. *J. Med. Chem.* **2020**, *63* (22), 13578–13594. https://doi.org/10.1021/acs.jmedchem.0c01170.

(99) Chen, Y.-N. P.; LaMarche, M. J.; Chan, H. M.; Fekkes, P.; Garcia-Fortanet, J.; Acker, M. G.; Antonakos, B.; Chen, C. H.-T.; Chen, Z.; Cooke, V. G.; Dobson, J. R.; Deng, Z.; Fei, F.; Firestone, B.; Fodor, M.; Fridrich, C.; Gao, H.; Grunenfelder, D.; Hao, H.-X.; Jacob, J.; Ho, S.; Hsiao, K.; Kang, Z. B.; Karki, R.; Kato, M.; Larrow, J.; La Bonte, L. R.; Lenoir, F.; Liu, G.; Liu, S.; Majumdar, D.; Meyer, M. J.; Palermo, M.; Perez, L.; Pu, M.; Price, E.; Quinn, C.; Shakya, S.; Shultz, M. D.; Slisz, J.; Venkatesan, K.; Wang, P.; Warmuth, M.; Williams, S.; Yang, G.; Yuan, J.; Zhang, J.-H.; Zhu, P.; Ramsey, T.; Keen, N. J.; Sellers, W. R.; Stams, T.; Fortin, P. D. Allosteric Inhibition of SHP2 Phosphatase Inhibits Cancers Driven by Receptor Tyrosine Kinases. *Nature* **2016**, *535* (7610), 148–152. https://doi.org/10.1038/nature18621.

(100) Montagner, A.; Yart, A.; Dance, M.; Perret, B.; Salles, J.-P.; Raynal, P. A Novel Role for Gab1 and SHP2 in Epidermal Growth Factor-Induced Ras Activation. *Journal of Biological Chemistry* **2005**, *280* (7), 5350–5360. https://doi.org/10.1074/jbc.M410012200.

(101) Bunda, S.; Burrell, K.; Heir, P.; Zeng, L.; Alamsahebpour, A.; Kano, Y.; Raught, B.; Zhang, Z.-Y.; Zadeh, G.; Ohh, M. Inhibition of SHP2-Mediated Dephosphorylation of Ras Suppresses Oncogenesis. *Nat Commun* **2015**, *6* (1), 8859. https://doi.org/10.1038/ncomms9859.

(102) Dance, M.; Montagner, A.; Salles, J.-P.; Yart, A.; Raynal, P. The Molecular Functions of Shp2 in the Ras/Mitogen-Activated Protein Kinase (ERK1/2) Pathway. *Cellular Signalling* **2008**, *20* (3), 453–459. https://doi.org/10.1016/j.cellsig.2007.10.002.

(103) Kontaridis, M. I.; Swanson, K. D.; David, F. S.; Barford, D.; Neel, B. G. PTPN11 (Shp2) Mutations in LEOPARD Syndrome Have Dominant Negative, Not Activating, Effects. *Journal of Biological Chemistry* **2006**, *281* (10), 6785–6792. https://doi.org/10.1074/jbc.M513068200.

(104) Bonham, C.; Mandati, V.; Singh, R.; Pappin, D.; Tonks, N. Coupling Substrate-Trapping with Proximity-Labeling to Identify Protein Tyrosine Phosphatase PTP1B Signaling Networks. *The Journal of Biological Chemistry* **2023**, 104582. https://doi.org/10.1016/j.jbc.2023.104582.

(105) Sha, F.; Kurosawa, K.; Glasser, E.; Ketavarapu, G.; Albazzaz, S.; Koide, A.; Koide, S. Monobody Inhibitor Selective to the Phosphatase Domain of SHP2 and Its Use as a Probe for Quantifying SHP2 Allosteric Regulation. *Journal of Molecular Biology* **2023**, *435* (8), 168010. https://doi.org/10.1016/j.jmb.2023.168010.